João Carlos Bernardo Oliveira Alves Santos

Licenciado em Ciências da Engenharia Eletrotécnica e de Computadores

3-D Hybrid Localization with RSS/AoA in Wireless Sensor Networks: Centralized Approach

Dissertação para obtenção do Grau de Mestre em

Engenharia Eletrotécnica e de Computadores

Orientador: Marko Beko, Professor Associado, Universidade Lusófona de Humanidades e Tecnologias

Co-orientador: Rui Dinis, Professor Associado com Agregação, Faculdade de Ciências e Tecnologia da Universidade Nova de Lisboa

FACULDADE DE CIÊNCIAS E TECNOLOGIA
UNIVERSIDADE NOVA DE LISBOA

September, 2016

3-D Hybrid Localization with RSS/AoA in Wireless Sensor Networks: Centralized Approach

"Mathematics, and perhaps mathematicians deal in the domain of the absolute and engineers live in the domain of the approximate. We are fundamentally interested in the practical. And so, frequently we make approximations, we cut corners, we omit terms and equations to get things that are simple enough to suit our purposes and our needs."

-Adam Stelzner,

American NASA engineer who works for the Jet Propulsion Laboratory

Acknowledgements

In this section I would like to take the opportunity to express my gratitude towards everyone who helped me through the process of developing and writing this dissertation.

First and foremost I would like to thank my adviser, Prof. Marko Beko, for his guidance, encouragement, and the enormous patience demonstrated over the last year.

I'm thankful to *Universidade Nova de Lisboa*, *Faculdade de Ciências e Tecnologia* and *Departamento de Engenharia Electrotécnica e de Computadores* for the opportunity and the conditions which allowed me to complete my education.

I would like to express my gratitude to Slavisa Tomic, a PhD student here at the university with many work done in this studied field, for his help in some crucial times.

To my dear colleagues and friends, specially, André Rosado, Diogo António, Tiago Dias and Francisco Cruz, thank you for always being there for me, through thick and thin. Without your friendship, support and motivation over the years, this journey would not have been the same.

And at last but not least, I would like to express my gratitude to my family, more specifically my mother and father, for all they have done that helped me become the man I am today. To my girlfriend Raquel, thank you for all the love and support, you have been the key person during this stage of my life.

Abstract

This dissertation addresses one of the most important issues present in Wireless Sensor Networks (WSNs), which is the sensor's localization problem in non-cooperative and cooperative 3-D WSNs, for both cases of known and unknown source transmit power P_T.

The localization of sensor nodes in a network is essential data. There exists a large number of applications for WSNs and the fact that sensors are robust, low cost and do not require maintenance, makes these types of networks an optimal asset to study or manage harsh and remote environments. The main objective of these networks is to collect different types of data such as temperature, humidity, or any other data type, depending on the intended application. The knowledge of the sensors' locations is a key feature for many applications; knowing where the data originates from, allows to take particular type of actions that are suitable for each case.

To face this localization problem a hybrid system fusing distance and angle measurements is employed. The measurements are assumed to be collected through received signal strength indicator and from antennas, extracting the received signal strength (RSS) and angle of arrival (AoA) information. For non-cooperative WSN, it resorts to these measurements models and, following the least squares (LS) criteria, a non-convex estimator is developed. Next, it is shown that by following the square range (SR) approach, the estimator can be transformed into a general trust region subproblem (GTRS) framework. For cooperative WSN it resorts also to the measurement models mentioned above and it is shown that the estimator can be converted into a convex problem using semidefinite programming (SDP) relaxation techniques.

It is also shown that the proposed estimators have a straightforward generalization from the known P_T case to the unknown P_T case. This generalization is done by making use of the maximum likelihood (ML) estimator to compute the value of the P_T.

The results obtained from simulations demonstrate a good estimation accuracy, thus validating the exceptional performance of the considered approaches for this hybrid localization system.

Keywords: AoA, GTRS, RSS, SDP, wireless localization, WSN.

Resumo

Esta dissertação aborda uma das temáticas mais importantes de Redes de Sensores Sem Fios (RSSFs),que consiste na localização de sensores em RSSFs 3-D não cooperativas e cooperativas. Para ambos os casos de quando se conhece e de quando se desconhece a potência de transmissão dos sensores P_T.

A localização dos sensores numa rede é um dado essêncial. Existe um grande número de aplicações possíveis para RSSFs e o facto de os sensores serem robustos, terem baixo custo e não terem necessidade de manutenção faz com que este tipo de redes seja uma óptima solução para estudar e gerir ambientes adversos e de difícil acesso. O principal objectivo deste tipo de redes é o de recolher dados como temperatura, húmidade, ou qualquer outro tipo de dados, dependente do tipo de aplicação a que se destina a rede. O conhecimento da localização dos sensores é uma característica fundamental para diversas aplicações porque ao se saber a localização do sensor, sabe-se a localização dos dados recolhidos e permite que determinadas acções possam ser tomadas com base na informação recolhida, variando de caso para caso.

Para fazer face a este problema de localização, implementou-se um sistema híbrido que combina medições de ângulos e distância. Assume-se que as medições são recolhidas através de um indicador de potência de sinal recebido e através de antenas, retirando a potência do sinal recebido e o ângulo de chegada do sinal. Para uma RSSF não-cooperativa, recorre-se a estes modelos de medições e seguindo o critério do *least squares* (LS), é desenvolvido um estimador não convexo. De seguida, mostra-se que seguindo a aproximação do *square range* (SR), o estimador pode ser transformado numa estrutura do tipo *general trust region subproblem* (GTRS). Para uma RSSF cooperativa recorre-se aos mesmos modelos de medições, referidos em cima, e é mostrado que o estimador pode ser convertido num problema convexo recorrendo-se à técnica de relaxação *semidefinite programming* (SDP).

Também é demonstrado que os estimadores propostos têm uma generalização direta do caso em que se conhece P_T para o caso em que não se conhece. Este generalização é feita recorrendo-se ao estimador *maximum likelihood* (ML) que é usado para calcular o valor da P_T.

Os resultados obtidos através das simulações realizadas demonstram a boa precisão na estimação da localização, validando o desempenho excecional das abordagens utilizadas para um sistema de localização híbrido.

Palavras-chave: Ângulo de chegada do sinal, GTRS, localização sem fios, potência do sinal recebido, RSSF, SDP.

Contents

List of Figures

List of Tables

Listings

Acronyms

AoA Angle of Arrival.

APIT Approximate Point In Triangulation.

APS Ad-Hoc Positioning System.

BR-PLE Bias Reduction Pseudolinear Estimator.

GPS Global Positioning System.

GTRS Generalized Trust Region Subproblem.

LS Least squares.

ML Maximum Likelihood.

NLOS Non Line Of Sight.

NRMSE Normalised Root Mean Square Error.

PDF Probability Density Function.

PLE Path Loss Exponent.

PPS Precise Positioning Service.

RF Radio Frequency.

RMSE Root Mean Square Error.

RSS Received Signal Strength.

RTT Round-Trip Time.

SDP Semidefinite Programming.

SDR Semidefinite Relaxation.

SOCP Second Order Cone Programming.

SOCR Second Order Cone Relaxation.

SPS Standard Position Service.

SR Square range.

SR-WLS Squared range weighted least squares.

TDoA Time Difference of Arrival.

ToA Time of Arrival.

WLS weighted least squares.

WSN Wireless Sensor Network.

Chapter 1

Introduction

1.1 Background and Motivation

Wireless Sensor Networks (WSNs) are a fairly explored theme, addressed and strongly consolidated in the literature that has been discussed over the past several years. The reason for that is related to the fact that there were huge advances in radio frequency and in electronics. Nowadays, the size of some components, constituting an integrated circuit (IC), are less than one millimetre making it possible to make smaller devices with the same, or even better, performance [1].

A WSN is built of sensor nodes, from a few to a large number of these small devices. The sensor nodes, generally spatially distributed trough a large area, are used to monitor different conditions such as temperature, sound, humidity or pressure, depending on their applications. They can be used to just sense the data or also to actuate somehow. The development of WSNs was motivated by military applications such as battlefield surveillance. This motivation is correlated with the fact that, in general, this type of network does not need infrastructures as the common applications use a sink node that collects all the data sensed by the sensors and it is that node which computes and performs the needed actions. The set up time and the implementation cost are also big advantages of using these networks [2].

These networks are commonly used in intelligent buildings to, for example, reduce energy wastage by proper ventilation, air conditioning or the needed illumination of a given room. They can also be used for smoke or fire detection in buildings. Other well known applications are the detection of wildfires over large forests or the study and observation of biodiversity in wildlife. Nowadays, with the automation in the industry, the WSNs are also used to help processes. The sensors may be used to detect equipment failures, sense data and, depending on the equipment, activate some actuators. Lately, the need of studying and monitoring oceans and rivers, led to new developments creating underwater and oceanographic WSNs in order to perform measurements far from the coastline, in the case of an oceanographic WSN, and to employ acoustic communications, pollution detection and to measure seismic activity in the case of underwater WSN [3].

As it has been seen, an infinity number of applications exists and the key feature for several of these applications consists in the location of the sensor which sensed some important data and consequently, an action is required. The main motivation for this dissertation is tied to the importance of knowing the sensors' locations. The location knowledge of a sensed data allows an improvement of the overall operation of a network. For example, lets consider an automated irrigation system for agriculture. Irrigating just the dry areas increases the overall efficiency and reduces wasteful spendings.

The global positioning system (GPS) is the most accurate localization system used worldwide, but it is not very common to use it in every sensor node of a WSN. This is due to the fact that requires high precision, a complex process of timing and synchronization, and it cannot operate at indoor applications [1]. Instead of this system and in order to get low-cost solutions, it is common to implement systems using different types of measurements, such as received signal strength (RSS), time of arrival (AoA), etc. The accuracy of these systems are much worse than a GPS-based localization system. Recently, instead of using just one type of the referred measurements, hybrid systems that fuse more than one type of these measurements were presented [4, 5, 6, 7]. These systems increase significantly the estimation accuracy while keeping the computational complexity low.

1.2 Dissertation Objectives

This dissertation addresses the sensors localization problem in a 3-D centralized WSN. The main goal is to analyse and evaluate a hybrid localization system performance using received signal strength (RSS) and angle of arrival (AoA) measurements. For that purpose, two schemes are considered: one non-cooperative and other cooperative localization. In each one, different estimators are developed with straightforward generalization from the cases of known source transmit power (P_T) to the cases of unknown source of transmit power (P_T).

The estimators considered in this work are expected to have a good accuracy over a wide noise range. On that basis, several simulations were performed in order to evaluate these estimators. A comparison, between the considered hybrid system with a different system using only one measurement type, is performed in every simulation in order to demonstrate the advantages of using this type of hybrid localization system instead of using other system with only one type of measurements.

1.3 Dissertation Outline

The remainder of this thesis is organized as follows: Chapter 2 contains a literature review that covers fundamental concepts and the state of the art related to the different concepts to be used throughout this dissertation. First, the main issues existing in WSNs are briefly described focusing on the sensors localization problem. The main concepts of classifications for localization schemes in WSNs are provided. Next, the GPS-based localization is introduced followed by the main alternatives consisting in major measurement models known and used in the literature. At the end of this chapter the concept of a hybrid localization scheme is given explaining the theoretical advantages of using it.

In Chapter 3 the localization problem that it is intended to be solved in this dissertation is formulated. The non-cooperative localization scheme, for both known and unknown source transmit power P_T, is presented and the steps needed to elaborate the developed estimators are explained. Next, the cooperative localization scheme, for both cases of known and unknown source transmitted power P_T, is addressed. It is shown how to transform the localization problem into a convex one and how this problem can be solved with convex optimization tools.

In Chapter 4, the computational complexity analysis of the considered algorithms in this dissertation is shown. Then, throughput evaluations were conducted through simulations of the proposed algorithms. A comparison between the estimators is performed and all the adopted considerations for the performed simulations are described.

Chapter 5 presents the final conclusions by highlighting the main contributions of this dissertation.

Chapter 2

State of the Art

2.1 Introduction

The purpose of this chapter is to establish a theoretical framework of this dissertation. In Section 2.2 the known problems of WSNs are presented, giving more attention to the localization problem and different possible schemes are explained. Next, the most commonly used measurement models that are employed to formulate the localization problem are shown in Section 2.4 giving more emphasis to the ones used in this dissertation in the following subsections.

At the end of this chapter, existing hybrid localization approaches, which use the measurements presented in 2.4, are presented.

2.2 Issues in WSNs

WSNs have several issues that affect their performance and design [8].The *Hardware* design must include a radio range as high as possible to ensure data connectivity; the *Operating System* should have inbuilt features to reduce the energy consumption; the *MAC protocols* should avoid collisions and other types of interferences thereby optimizing the energy consumption of sensors; the *Synchronization protocol* is needed to be robust to delays, in the communication process, and failures. When the *Deployment* is random, as for example, the sensors are dropped by a plane in a harsh environment, despite of a short distance between two deployed sensors, they can be unable to communicate due to obstacles or interferences. To maximize the energy efficiency, the *Network Layer* should provide a flexible platform to perform routing and data management. The *Transport Layer* should have protocols that ensure the transmission order of fragmented segments.

These are some of the known problems that reside in WSNs. But one of the most important problems, not mentioned above, in these type of networks is the knowledge of the *Localization* of the sensors. This is the main topic of this dissertation and is described with more detail in the next section 2.3.

2.3 Localization Problem

The localization theme is a crucial issue in WSNs management and operation. The localization procedure is defined as the task of determining the physical coordinates of a sensor node (or a group of sensor nodes) or the spatial relationship between nodes [1]. Without the knowledge of the sensors location, the sensed data can be meaningless in many applications. For example, in an irrigation system if it is not known which part of the ground needs to be watered, the whole crop can be spoiled. On the other hand, in a wildfire detection, if the sensor location, which detected the fire, is known, the responsible entities could act more quickly and efficiently.

There are several classifications for localization schemes. A network can be centralized or distributed, cooperative or non-cooperative, the sensor nodes can be mobile or stationary, the localization algorithms may be anchor-based or anchor-free and range-based or range-free. These classifications are described with more detail below.

2.3.1 Stationary and mobility in sensor nodes

Most of the applications in WSNs uses static nodes, which means that, after their deployment, they stay stationary. Mobile sensors require specific algorithms and due to there complexity, less designed mechanisms exist [9]. When compared static with mobile nodes, it is perceptible that for a static node, its location is computed only one time. However, for mobile nodes, due to their movement, the algorithms have to adapt and perform the location estimation at every moment, depending on the application.

2.3.2 Centralized and de-centralized networks

The localization schemes can be classified as *centralized*, where information is passed to a central node, or *distributed* where all sensors estimate their own positions. In a centralized scheme, computation is left for a central node, implying high energy efficient schemes. A de-centralized or distributed scheme requires that each node processes its own data, thus increasing the energy consumption of the entire network [10].

2.3.3 Anchor-based and anchor-free algorithms

Other typical classification for localization schemes is if an algorithm is *anchor-based* or *anchor-free*. An *anchor* is a sensor node who is aware of its location through manual configuration or using GPS. In an anchor-based algorithm anchors correspond to a small percentage of the nodes constituting a network and they are used to estimate the unknown location of the other sensors (*targets*). In an anchor-free algorithm, instead of a global positioning of the nodes, one coordinate system must be established by a reference group of nodes [11].

For the sake of simplicity, in the remainder of the text, the sensors with known location will be called *anchors* and the sensors with unknown location *targets*.

2.3.4 Cooperative and non-cooperative networks

Considering a WSN constituted by anchors and targets, in a non-cooperative scenario each target only communicates with anchors, and each position is estimated at a time. On the other scenario, node cooperation allows direct communication between any two nodes which are within the communication range, and all targets are localized simultaneously [12].

For networks with few energy resources, where only some targets can communicate directly with anchor nodes, a node cooperation is necessary. This is also made to extend the sensors lifetime [13].

2.3.5 Range-based and range-free localization

The algorithms for nodes position estimation are divided in two major classes, *range-free* and *range-based* localization algorithms.

A **range-free** localization uses the radio connectivity among nodes in order to infer their position instead of using distance or angle measurements as in range-based localization. The main techniques used for this type of localization are the *Ad-Hoc Positioning System (APS)*, *Centroid System*, *Gradient* and *Approximate Point in Triangulation (APIT)*, which are briefly presented in the following [1, 10, 14, 15].

The APS can use the *DV-hop* method to estimate a target position [16]. This method (Fig. 2.1) is based on the distance vector protocol and the position estimation is done using hop count. To determine targets position, the anchors flood the network with their coordinates, generally obtained via GPS, and a hop count, which is incremented at each neighbour. Then, a correction factor is calculated in case an anchor obtains distances to another anchor. Having the anchors location and the correction factor, a target can perform its location estimation using trilateration, which will be discussed further.

The Centroid System (Fig. 2.2) presented in [17] uses multiple anchors to compute the target position. The anchors location are given to the target and its position is estimated as being the center of those multiple anchors.

In the Gradient algorithm presented in [18], anchors initiate a gradient that self-propagates and allow the target to estimate its distance from the anchor. Every target obtain informations of the shortest path from the anchors. The location of the target is computed through multilateration after estimating the distances from three different anchors.

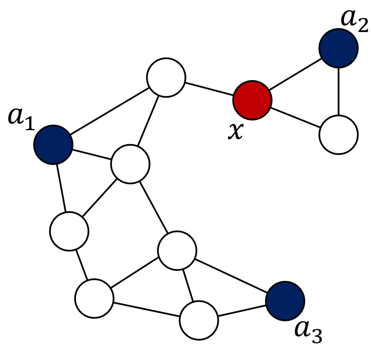

Figure 2.1: DV-Hop

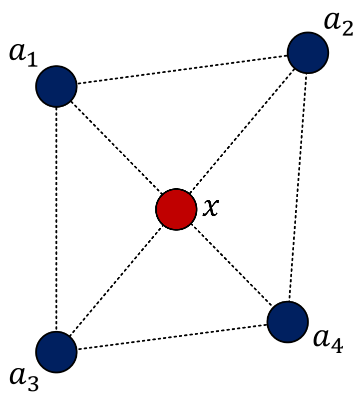

Figure 2.2: Centroid System

The APIT (Fig. 2.3), proposed in [14], requires a heterogeneous network where a small percentage of the devices are anchors equipped with high-power transmitters. The anchors form triangular regions between them and a target's presence inside or outside these regions allow the target to refine down the area in which it can potentially remain.

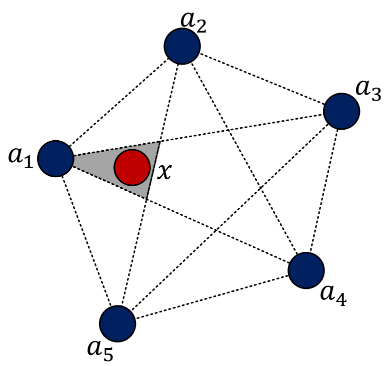

Figure 2.3: APIT

A **range-based** localization uses range measurements such as *Time of Arrival (ToA)*, *Time Difference of Arrival (TDoA)*, *Received Signal Strength (RSS)* or *Angle of Arrival (AoA)*, outlined in Section 2.4. Range-free localization techniques do not require additional hardware and are therefore a cost-effective alternative to these techniques. But the trade-off between cost and accuracy is an important factor and the range-based techniques are more appropriated to scenarios where the localization accuracy is a fundamental factor.

The concepts commonly used to estimate sensors locations in this type of localization are based on *Triangulation*, Fig. 2.4, which measures the angles from more than one anchor using AoA; *Trilateration*, Fig. 2.5, which measures the distance from three different anchors using RSS, ToA or TDoA; and *Multilateration*, which is equal to the latter but where more than three anchors are used [1, 10]. In theory, the exact location is found

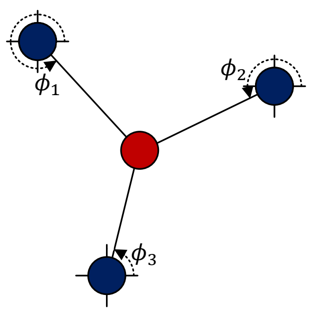

Figure 2.4: Triangulation

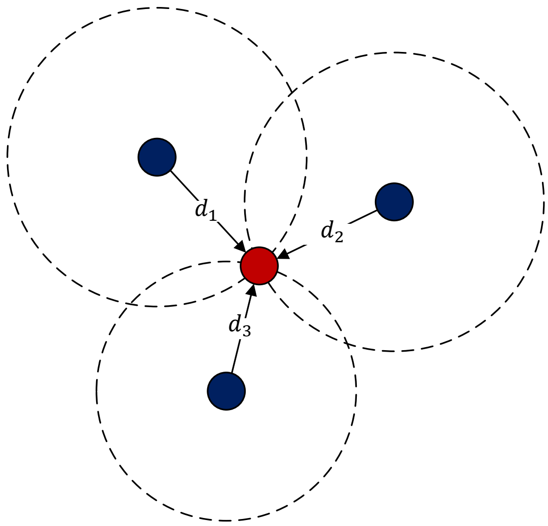

Figure 2.5: Trilateration

with one of those concepts, but in the real world, measurement errors occur due to the surrounding noise. This may lead to inaccurate localization and the need of an algorithm to solve this problem emerge.

GPS-based Localization

Global Positioning System (GPS) is the most well known localization technique used worldwide. Initially developed by United States Department of Defense (DoD) under the name NAVSTAR (Navigation Satellite Timing and Ranging) for military purposes, nowadays, the GPS has two levels of service [1].

1. Standard Position Service (SPS) which is a free positioning service available for civilian purposes. Tracking, surveillance and navigation, among many other applications, using high quality GPS receivers based on SPS are capable of achieving precision of three meters.

2. Precise Positioning Service (PPS) which is intended to serve the US and Allied military users with a more robust service that includes encryption and jam resistance. Instead of one signal, as SPS, the PPS uses two signals to reduce errors.

To obtain its location, a GPS receiver needs to have four satellites in line of sight. Each satellite broadcasts information with its own location, identity, status and the date and time of the signal sent under coded radio waves. The receiver and the satellites use very precise and synchronized clocks in order to generate at the same code exactly the same time. Comparing the generated code by the receiver with the one received by the satellite, the time of the travelled code is discovered and knowing that the radio waves travel at the speed of light, the distance between them can be determined based on ToA. The Fig. 2.6 represents this principle. After the receiver calculates its distance from each satellite, multilateration is used to obtain an accurate location.

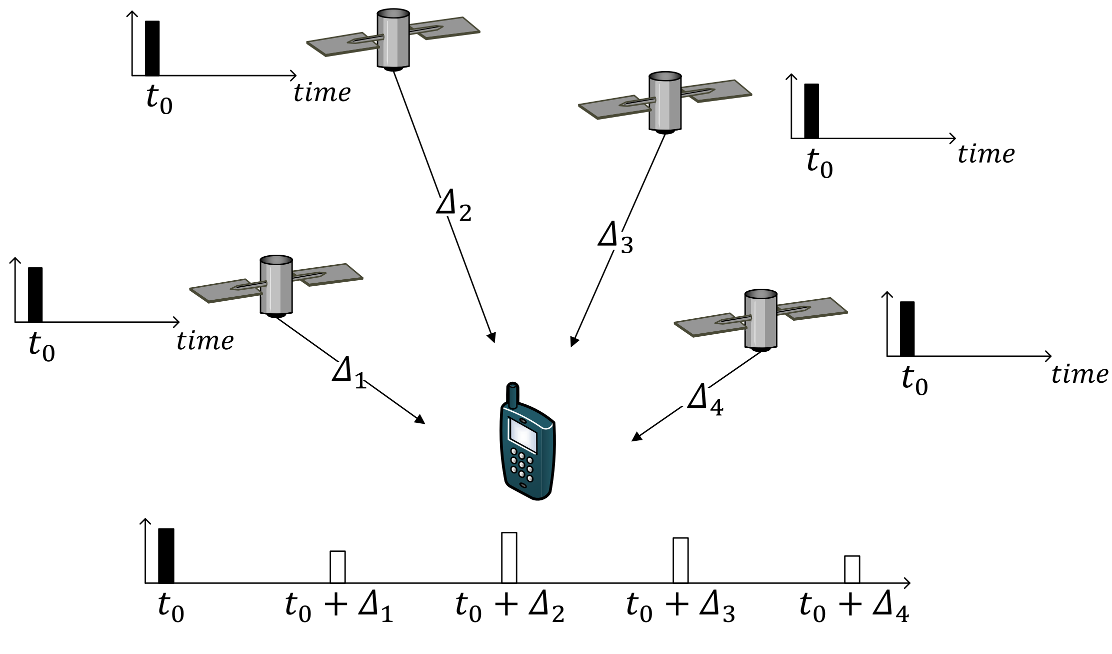

Figure 2.6: GPS-based localization principle

The GPS receiver has several constraints for its use in every sensor of a WSN. The high power consumption is a major issue that affects the lifetime of each sensor; its cost could make an entire network unaffordable and is limited to outdoor applications because of its need for line of sight. In order to maintain low implementation costs, only a small fraction of sensors are equipped with GPS receivers (called anchors), while the remaining ones (called targets) determine their locations by using a kind of localization scheme that takes advantage of the known anchor locations.

2.4 Measurement Models

This section summarizes the several types of measurement models used in range-based localization, giving more focus to the ones used in this dissertation. These models are required to formulate the localization problems and their usage depends on the available hardware.

2.4.1 RSS Model

It is known by [1, 19] that, a signal decays with the travelled distance following a power law of the separating length between sensors. The average received power P_{ij} at i-th sensor with a distance d_{ij} from the j-th sensor, is approximated by

$$P_{ij} = P_0 \left(\frac{d_{ij}}{d_0} \right)^{-\gamma}, \tag{2.1}$$

or

$$P_{ij}(dB) = P_0(dB) - 10\gamma \log_{10} \left(\frac{d_{ij}}{d_0} \right), \tag{2.2}$$

where P_0 is the received power at a short reference distance d_0 and γ is the path loss exponent (PLE), typically ranged between 2 and 4 [20, 21]. In table 2.1 are shown the different values for PLE.

Table 2.1: Path Loss Exponents for Different Environments [19]

Environment	Path Loss Exponent (PLE), γ
Free space	2
Urban area cellular radio	2.7 to 3.5
Shadowed urban cellular radio	3 to 5
In building line-of-sight	1.6 to 1.8
Obstructed in building	4 to 6
Obstructed in factories	2 to 3

The equation (2.2) can be rewritten as

$$P_{ij}(dB) = P_0(dB) - 10\gamma \log_{10} \left(\frac{d_{ij}}{d_0} \right) + X_\sigma, \tag{2.3}$$

for simulation purposes, where X_σ reflects the signal attenuation caused by fading, which is explained with more detail in the next sub-subsection 2.4.1.1.

Because of its low complexity and cost in software and hardware implementations, RSS is a popular method among the different types of measurements [22].

In [23] the authors proposed a weighted least squares (WLS) method when the source transmit power of a sensor and the PLE are unknown. In [24] to estimate the source transmit power along with the target's location in a cooperative scenario, the authors resorted to a Semidefinite Programming (SDP) technique, which is a class of convex optimization. These are two examples of the research work in WSNs using the RSS model in the recent years.

Besides the type of ranging technique used to solve the localization problem it is necessary to appeal to mathematical models to compute the sensors location.

2.4.1.1 Log-Distance Path Loss Model

Path loss is a very important model in a wireless or radio communication system because it describes the signal attenuation between a transmit and receiver antenna (e.g. two sensors i and j) due to multipath and shadowing caused by obstructions. Path loss model (in dB) is described as follows [19]

$$L_{ij}(dB) = 10\log_{10}\frac{P_T}{P_{ij}}, \tag{2.4}$$

where L_{ij} is the path loss of the propagation channel between the sensors i and j, P_T is the transmission power and P_{ij} is the average received power between sensors. Replacing this equation in the RSS measurement model (2.2), the *Log-distance Path Loss Model* is obtained

$$L_{ij}(dB) = L_0(dB) + 10\gamma\log_{10}\left(\frac{d_{ij}}{d_0}\right), \tag{2.5}$$

where L_0 represents the path loss at the short reference distance of d_0 [19].

It has been showed in [25, 26] that the path loss at any distance d_{ij} in a same place is random and log-normally distributed about the mean distance-dependent value. So, in addition to this model, it is added a *Log-normal Shadowing* term to consider the facts mentioned above, resulting in the equation

$$L_{ij}(dB) = L_0(dB) + 10\gamma\log_{10}\left(\frac{d_{ij}}{d_0}\right) + X_\sigma, \tag{2.6}$$

where X_σ is a zero-mean normal (Gaussian) distributed random variable with standard deviation σ and is denoted by

$$X_\sigma \sim \mathcal{N}\left(0, \sigma^2\right). \tag{2.7}$$

As previously evidenced, the passage of the RSS model (2.3) to the log-distance path loss model (2.6) is straightforward, however, many authors use this latter model, as an alternative, to obtain their distance measurement through the RSS.

In [27], the authors investigated the noncooperative and cooperative schemes obtaining the location estimation of the targets through SDP estimators. For indoor localization, the authors in [28] used a WLS approach for cooperative and noncooperative schemes. However, to solve the localization problem, in the first scenario they relaxed that approach as a mixed semidifinite and second-order cone programming (SD/SOCP) and in the second they solved the WLS approach through the bisection method. In [12], the authors also investigated the noncooperative and cooperative localization problems for known and unknown source transmitted power based on a SOCP approach.

2.4.2 AoA Model

By definition, AoA is the angle measured between two sensors. To use this type of measurement it is necessary to equip the sensors with either a directional antenna or multiple antennas [29].

In a 3-D scenario, two types of angles are needed: *azimuth* and *elevation* (Fig. 2.7). A 2-D scenario only has two coordinates so, an elevation measure is not needed.

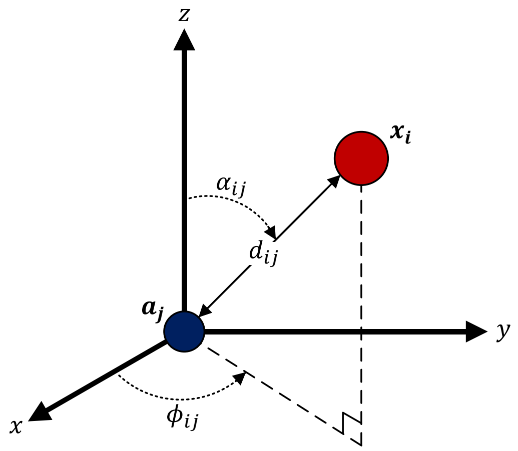

Figure 2.7: 3-D scenario illustration using AoA measurement

where x_i represents the i-th target node with unknown coordinates $[x_{i1}\ x_{i2}\ x_{i3}]$, a_j the j-th anchor node with known coordinates $[a_{j1}\ a_{j2}\ a_{j3}]$, ϕ_{ij} is the azimuth angle, α_{ij} is the elevation angle and d_{ij} is the real distance between the nodes.

It can be readily shown, from Fig. 2.7, that the formulas for azimuth and elevation angles are, respectively

$$\phi_{ij} = \arctan\left(\frac{x_{i2} - a_{j2}}{x_{i1} - a_{j1}}\right) + m_{ij}, \tag{2.8}$$

and

$$\alpha_{ij} = \arccos\left(\frac{x_{i3} - a_{j3}}{d_{ij}}\right) + n_{ij}, \tag{2.9}$$

where m_{ij} and n_{ij} are introduced to represent possible measurement errors of both angles.

In [30], the authors studied a 3-D scenario and proposed a method called bias reduction pseudolinear estimator (BR-PLE) to estimate the sensor position. This approach jointly with [31, 32, 33, 34, 35], are some of the research work made with 3-D measurements of AoA. The 2-D scheme is very well substantiated in [36, 37, 38, 39, 40, 41].

2.4.3 ToA Model

The ToA is based on a simple law of physics stating that the distance between two sensors (e.g. an anchor and a target) can be obtained using the measured signal propagation time and its velocity [1, 42]. To do this, as was seen in GPS, both sensors need very accurate and synchronized clocks which increases the complexity and cost of the network. There are two different ranging schemes for this method.

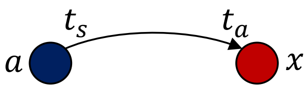

Figure 2.8: One-way ToA

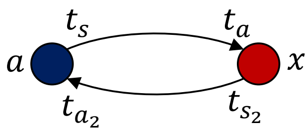

Figure 2.9: Two-way ToA

The *one-way* ToA (Fig. 2.8) (used in GPS) measures the propagation time between the sensors computed as being the difference among the sending (t_s) and arrival time (t_a) of the signal. The other possibility is to use the *two-way* ToA (Fig. 2.9) which measures the round-trip time (RTT) of the signal. The measured distances by these two methods, respectively, are computed as follows

$$d_{ij} = (t_a - t_s) \times v, \tag{2.10}$$

and

$$d_{ij} = \frac{(t_{a2} - t_s) - (t_{s2} - t_a)}{2} \times v, \tag{2.11}$$

where d_{ij} is the distance between the i-th anchor and the j-th target, the variables t represent the times of sending and arrival signal and v is the velocity of the signal which is known, just depends on what type of signal is propagated (RF, acoustic or other).

Beyond these differences, with the one-way ToA, the target can compute its own position because it estimates the distance between the target and the anchor (equation (2.10)). In the two-way ToA it is the anchor who estimates the distance among them (equation (2.11)) forcing a third message to be sent so that the target can compute its own location.

The approach of [43] considers non line of sight (NLOS) conditions and the authors proposed two relaxation methods based on semidefinite relaxation (SDR) and second order cone relaxation (SOCR) for two different cases where NLOS status is or is not known.

2.4.4 TDoA Model

The TDoA representation (Fig. 2.10) uses two different types of signals, that travel with different velocities [1, 44]. Both signals can be sent at a same time or after a fixed interval (t_w). The distance between the anchor and the target is determined by the latter (equation (2.12))

$$d_{ij} = |v_1 - v_2| \times (t_{a2} - t_a - t_w), \tag{2.12}$$

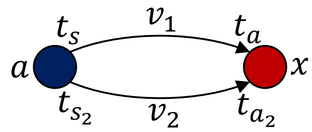

Figure 2.10: TDoA

where the variables v represent the different velocities of the signals, t_a and t_{a2} are the times of arrival of the signals and t_w is the time difference between the sent signals ($t_w = t_{s2} - t_s$).

When compared to ToA, this method has the advantage of not needing clock synchronization between targets and anchors, but has the disadvantage that is required additional hardware depending of the different signal types used. Similarly to one-way ToA and opposed to two-way ToA, in TDoA is the unknown target that estimate its own position.

2.5 Hybrid Localization

Due to measurement errors in each individual ranging technique, a hybrid localization scheme is thought to improve the localization performance by fusing more than one measurement type. A hybrid system has more available information, and by exploiting this information, a better accuracy in the localization procedure can be obtained. On the other hand, combining measurements implies an increased complexity of network devices increasing the network implementation costs [22, 42]. There are many possible schemes studied in the literature which are presented further in this section. Next, the hybrid localization scheme which uses RSS and AoA measurements is presented, since it is the main technique applied for this dissertation.

The range measurements can be obtained exclusively from RSS (Fig. 2.11) which has errors associated to the shadowing term. The angle measurements may be obtained through AoA (Fig. 2.12) which has associated errors given by antennas and digital compasses due to its static accuracy. In the above mentioned figures, $\hat{d_i}$ represents each range measurement, of an anchor, defining a circle as a possible location of the unknown target. Hence, a set of range measurements defines multiple circles and their intersected area contains a set of the target possible locations. Similarly, each angle measurement, ϕ_i, defines a line as the set of possible locations of the unknown target.

As it can be seen, both figures (Fig. 2.11 and Fig. 2.12) have a set of target possible locations, given by real conditions instead of an accurate and theoretical position estimation as shown in Fig. 2.4 and Fig. 2.5 where measurement errors are not considered. When used in conjunction, an improved performance is obtained as it can be seen from Fig. 2.13

In Fig. 2.13 one can see that when both measurements are integrated, the set of

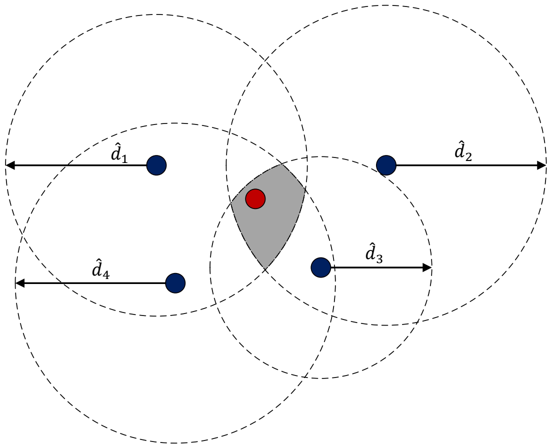

Figure 2.11: Range-based Localization

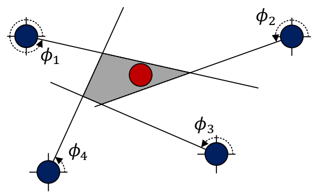

Figure 2.12: Angle-based Localization

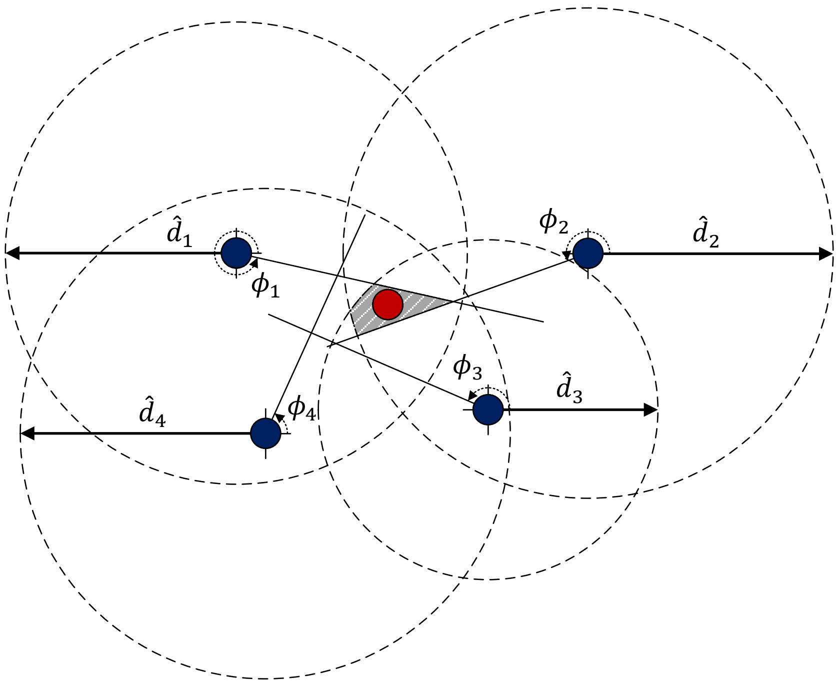

Figure 2.13: Hybrid Localization in a 2-D scenario using RSS/AoA

possible solutions for the target's location is reduced, proofing that hybrid systems are more likely to improve the estimation accuracy [45]. In this dissertation, the hybrid RSS/AoA system is employed but instead of 2-D, a 3-D scenario is used.

The authors in [6] proposed a selective weighted least squares (WLS) estimator for a RSS/AoA localization problem in a 2-D scenario for a non-cooperative network. By exploiting weighted ranges from the nearest anchors combined with the AoA measurements, they determined the unknown target location. In [46] the authors presented a WLS estimator for a 3-D non-cooperative localization problem using RSS difference fused with AoA measurements. In [4, 5, 6] the authors only studied the hybrid RSS/AoA system for localization problem in a 2-D non-cooperative scenario only.

Other combinations of measures for hybrid localization systems are also studied in the literature. In [7, 47, 48] the authors made their approaches based on the combination between RSS and the two-way ToA measurements.

In [49], the authors introduced a new concept in hybrid localization. They combined a range-based with a range-free attribute, being the RSS and the DV-Hop the choices made to perform the unknown target localization in a 3-D scenario.

CHAPTER 3

Hybrid Localization System Implementation

3.1 Introduction

In Section 3.2 the mathematical models to obtain the distance and angle measurements are presented for both cases of cooperative and non-cooperative scenarios and the target localization problem is formulated. Next, in section 3.3 the hybrid localization system implementation is addressed for the non-cooperative scenario for both cases of known and unknown source transmit power P_T. This chapter ends with the presentation of the proposed algorithm for the cooperative scenario.

3.2 Problem Formulation

A WSN with N anchors and M targets is considered, where the anchors and the unknown targets locations are denoted, respectively, by

$$\boldsymbol{a}_j \in \mathbb{R}^3,\ \forall\ j = 1, 2, \ldots, N, \qquad \boldsymbol{x}_i \in \mathbb{R}^3,\ \forall\ i = 1, 2, \ldots, M.$$

To determine the unknown targets location, a hybrid system fusing distance and angle measurements is employed in a 3-D scenario. Each sensor node has three coordinates (x, y and z) represented as

$$\boldsymbol{a}_j = [a_{j1}\ a_{j2}\ a_{j3}],\ \forall\ j = 1, 2, \ldots, N, \qquad \boldsymbol{x}_i = [x_{i1}\ x_{i2}\ x_{i3}],\ \forall\ i = 1, 2, \ldots, M.$$

The range measurements in this dissertation are assumed to be obtained exclusively through RSS information, more precisely, through the log-distance path loss model given in the previous chapter by equation (2.6). This assumption is made based on the fact that ranging based on RSS requires the lowest implementation costs. In this work, there are two different connections types, the target/anchor connection, which form a set $\mathcal{A}$, and the target/target connection, which form a set $\mathcal{B}$. These sets are described as follows

$$\mathcal{A} = \{(i,j) : \|\boldsymbol{x}_i - \boldsymbol{a}_j\| \leq R, \ \forall\ i = 1,2,\ldots,M,\ j = 1,2,\ldots,N\},$$

and

$$\mathcal{B} = \{(i,k) : \|\boldsymbol{x}_i - \boldsymbol{x}_k\| \leq R, \ \forall\ i,k = 1,2,\ldots,M,\ i \neq k\},$$

where R represents the communication range of any sensor of the network, $\boldsymbol{x}_i$ and $\boldsymbol{x}_k$ are the i-th and k-th unknown targets and $\boldsymbol{a}_j$ is the $j-th$ anchor. The norms $\|\boldsymbol{x}_i - \boldsymbol{a}_j\|$ and $\|\boldsymbol{x}_i - \boldsymbol{x}_k\|$ are the Euclidean norms and represent the distance between the two involved sensors.

Based on the sets mentioned above, the log-distance path loss model for each of set are modelled as:

$$L_{ij}^{\mathcal{A}} = L_0 + 10\gamma \log_{10}\left(\frac{\|\boldsymbol{x}_i - \boldsymbol{a}_j\|}{d_0}\right) + n_{ij},\ \forall\ (i,j) \in \mathcal{A}, \tag{3.1a}$$

and

$$L_{ik}^{\mathcal{B}} = L_0 + 10\gamma \log_{10}\left(\frac{\|\boldsymbol{x}_i - \boldsymbol{x}_k\|}{d_0}\right) + n_{ik},\ \forall\ (i,k) \in \mathcal{B}, \tag{3.1b}$$

where n_{ij} and n_{ik} are the log-normal shadowing terms modelled as zero-mean normal (Gaussian) distributed random variables with standard deviation (σ_{ij} and σ_{ik} respectively). The distance between sensors must meet the constraint of being equal or greater than the short reference distance (d_0) of a sensor.

In the rest of this work, without loss of generality, an assumption is made that the target/target path loss measurements, are symmetric, meaning that $L_{ik} = L_{ki}\ \forall\ i \neq k$.

After obtaining the RSS or the path loss measurements, is possible to estimate the distance between sensors. Knowing that the errors in equation (3.1a) and (3.1b) are represented by a random variable with zero-mean, the estimated distance for each set of sensors is given by

$$\hat{d}_{ij}^{\mathcal{A}} = d_0 10^{\frac{L_{ij}^{\mathcal{A}} - L_0}{10\gamma}},\ \forall\ (i,j) \in \mathcal{A}, \tag{3.2a}$$

and

$$\hat{d}_{ik}^{\mathcal{B}} = d_0 10^{\frac{L_{ik}^{\mathcal{B}} - L_0}{10\gamma}},\ \forall\ (i,k) \in \mathcal{B}. \tag{3.2b}$$

The estimated distance in equation (3.2a) and (3.2b) can also be achieved through the maximum likelihood (ML) estimator [42].

The angle measurements needed for the 3-D scenario (azimuth and elevation) are obtained through AoA model which needs additional hardware as mentioned before. Applying the equation (2.8), for azimuth angle, to sets $\mathcal{A}$ and $\mathcal{B}$ results in

$$\phi_{ij}^{\mathcal{A}} = \arctan\left(\frac{x_{i2} - a_{j2}}{x_{i1} - a_{j1}}\right) + m_{ij},\ \forall\ (i,j) \in \mathcal{A}, \tag{3.3a}$$

and

$$\phi_{ik}^{\mathcal{B}} = \arctan\left(\frac{x_{i2} - x_{k2}}{x_{i1} - x_{k1}}\right) + m_{ik}, \ \forall \ (i,k) \in \mathcal{B}, \tag{3.3b}$$

where m_{ij} and m_{ik} are noise terms. These terms, coming from two different sources, are the angle measurement errors and the orientation errors.

Similarly, when the equation (2.9) is applied for elevation angle, also to both sets, it results in

$$\alpha_{ij}^{\mathcal{A}} = \arccos\left(\frac{x_{i3} - a_{j3}}{||\boldsymbol{x}_i - \boldsymbol{a}_j||}\right) + v_{ij}, \ \forall \ (i,j) \in \mathcal{A}, \tag{3.4a}$$

and

$$\alpha_{ik}^{\mathcal{B}} = \arccos\left(\frac{x_{i3} - x_{k3}}{||\boldsymbol{x}_i - \boldsymbol{x}_k||}\right) + v_{ik}, \ \forall \ (i,k) \in \mathcal{B}, \tag{3.4b}$$

where v_{ij} and v_{ik} are the same type of errors as the ones appearing in the equations (3.3a) and (3.3b) for the azimuth angle.

Although the errors stem from different sources, without loss of generality, they are modelled as one random variable [29]. The errors of azimuth and elevation angle are modelled as follows

$$\begin{cases} m_{ij} \sim \mathcal{N}\left(0, {\sigma_{m_{ij}}}^2\right), \\ m_{ik} \sim \mathcal{N}\left(0, {\sigma_{m_{ik}}}^2\right). \end{cases} \qquad \begin{cases} v_{ij} \sim \mathcal{N}\left(0, {\sigma_{v_{ij}}}^2\right), \\ v_{ik} \sim \mathcal{N}\left(0, {\sigma_{v_{ik}}}^2\right). \end{cases}$$

These different measures, comprehending the estimated distances ($\hat{d}_{ij}^{\mathcal{A}}$ and $\hat{d}_{ik}^{\mathcal{B}}$), the estimated azimuth angles ($\phi_{ij}^{\mathcal{A}}$ and $\phi_{ik}^{\mathcal{B}}$) and the estimated elevation angles ($\alpha_{ij}^{\mathcal{A}}$ and $\alpha_{ik}^{\mathcal{B}}$), are needed for all the investigated cases and only after their acquisition is possible to develop algorithms to estimate the unknown targets location. The combination of these measurements is the foundation of the hybrid system implementation.

Resorting to the equations presented in (3.1), (3.3) and (3.4), the observation vector is given as:

$$\boldsymbol{\theta} = \left[\boldsymbol{L}^T, \boldsymbol{\theta}^T, \boldsymbol{\alpha}^T\right] \quad , \left(\boldsymbol{\theta} \in \mathbb{R}^{3(|\mathcal{A}|+|\mathcal{B}|)}\right),$$

where $\boldsymbol{L} = \left[L_{ij}^{\mathcal{A}}, L_{ik}^{\mathcal{B}}\right]^T$, $\boldsymbol{\phi} = \left[\phi_{ij}^{\mathcal{A}}, \phi_{ik}^{\mathcal{B}}\right]^T$, $\boldsymbol{\alpha} = \left[\alpha_{ij}^{\mathcal{A}}, \alpha_{ik}^{\mathcal{B}}\right]^T$, and $|\mathcal{A}|$ and $|\mathcal{B}|$ denotes the number of elements in each set. Having the observation vector, the probability density function (PDF) is easily obtained as:

$$p(\boldsymbol{\theta} \mid \boldsymbol{x}) = \prod_{i=1}^{3(|\mathcal{A}|+|\mathcal{B}|)} \frac{1}{\sqrt{2\pi{\sigma_i}^2}} \exp\left\{-\frac{(\boldsymbol{\theta}_i - f_i(\boldsymbol{x}))^2}{2{\sigma_i}^2}\right\} \tag{3.5}$$

where

$$\boldsymbol{f}(\mathbf{x}) = \begin{bmatrix} \vdots \\ L_0 + 10\gamma \log_{10}\left(\frac{\|\boldsymbol{x}_i - \boldsymbol{a}_j\|}{d_0}\right) \\ \vdots \\ L_0 + 10\gamma \log_{10}\left(\frac{\|\boldsymbol{x}_i - \boldsymbol{x}_k\|}{d_0}\right) \\ \vdots \\ \arctan\left(\frac{x_{i2} - x_{k2}}{x_{i1} - x_{k1}}\right) \\ \vdots \\ \arctan\left(\frac{x_{i2} - x_{k2}}{x_{i1} - x_{k1}}\right) \\ \vdots \\ \arccos\left(\frac{x_{i3} - a_{j3}}{\|\boldsymbol{x}_i - \boldsymbol{a}_j\|}\right) \\ \vdots \\ \arccos\left(\frac{x_{i3} - x_{k3}}{\|\boldsymbol{x}_i - \boldsymbol{x}_k\|}\right) \\ \vdots \end{bmatrix}, \qquad \boldsymbol{\sigma} = \begin{bmatrix} \vdots \\ \sigma_{n_{ij}} \\ \vdots \\ \sigma_{n_{ik}} \\ \vdots \\ \sigma_{m_{ij}} \\ \vdots \\ \sigma_{m_{ik}} \\ \vdots \\ \sigma_{v_{ij}} \\ \vdots \\ \sigma_{v_{ik}} \\ \vdots \end{bmatrix}.$$

The ML estimator is the most popular approach since it has the property of being asymptotically efficient for enough data records allowing it to be implemented for complicated estimation problems [50]. The conditional PDF, presented in (3.5) is maximized through the following ML estimator:

$$\hat{\boldsymbol{x}} = \arg\min_{\boldsymbol{x}} \sum_{i=1}^{3(|\mathcal{A}|+|\mathcal{B}|)} \frac{1}{\sigma_i^2} \left[\theta_i - f_i(\boldsymbol{x})\right]^2, \tag{3.6}$$

where $\hat{\boldsymbol{x}}$ is the resulting array from the ML estimation.

Although the ML estimator is approximately the minimum variance unbiased estimator [50], the LS problem presented in (3.6) is non-convex and has no closed-form solution. The main goal of this dissertation is to apply certain approximations so that it is possible to solve the localization problem presented in (3.6) in an efficient manner. For non-cooperative WSN a non-convex estimator is proposed and for the case of cooperative WSN a convex one is proposed. These approaches, which are described with more detail in the following sections, not only efficiently solve the traditional RSS/AoA localization problem, but they also can be used to solve the localization problem when P_T is unknown with a straightforward generalization.

3.3 Non-Cooperative Localization

In a non-cooperative localization scenario for WSN, comprising targets and anchors, the targets are only able to communicate with anchors, and one single target is located at a time. For this type of configuration, it is assumed that the targets are passive nodes, which means that the sensors only report information, without processing it, through the emission of radio waves, and the anchors are the sensor nodes that collect all the radio measurements.

As the targets communicate exclusively with anchors, the set $\mathcal{B}$ is empty, so the equations (3.1b), (3.2b), (3.3b) and (3.4b) to calculate, respectively, the path loss, the approximated distance, the azimuth and the elevation angles for this set are not used in a non-cooperative localization scheme. For this type of scenario, it is assumed that the communication range (R) is high enough so that it is possible that the target can communicate with every anchor in the network.

To solve the localization problem presented in equation (3.6), a suboptimal estimator is developed, obtaining the exact solution through a bisection method. This estimator and the method are explained with more detail in the following subsections.

3.3.1 Known source transmit power (P_T)

For the case when the P_T is known, the first step is to assume that when the noise power is small enough, the following equations are obtained:

$$\lambda_{ij}^{\mathcal{A}} \|\boldsymbol{x}_i - \boldsymbol{a}_j\| \approx d_0, \ \forall \ (i,j) \in \mathcal{A}, \tag{3.7}$$

$$\boldsymbol{c}_{ij}{}^T \left(\boldsymbol{x}_i - \boldsymbol{a}_j\right) \approx 0, \ \forall \ (i,j) \in \mathcal{A}, \tag{3.8}$$

$$\boldsymbol{k}_{ij}{}^T \left(\boldsymbol{x}_i - \boldsymbol{a}_j\right) \approx \|\boldsymbol{x}_i - \boldsymbol{a}_j\| \cos\left(\alpha_{ij}^{\mathcal{A}}\right), \ \forall \ (i,j) \in \mathcal{A}, \tag{3.9}$$

where $\lambda_{ij}^{\mathcal{A}} = 10^{\frac{L_0 - L_{ij}^{\mathcal{A}}}{10\gamma}}$, $\boldsymbol{c}_{ij} = [-\sin\left(\phi_{ij}^{\mathcal{A}}\right),\ \cos\left(\phi_{ij}^{\mathcal{A}}\right),\ 0]^T$ and $\boldsymbol{k}_{ij} = [0,\ 0,\ 1]^T \ \forall (i,j) \in \mathcal{A}$. The next step consists in squaring both sides of equation (3.7) resulting in

$$\lambda_{ij}^{\mathcal{A}\,2} \|\boldsymbol{x}_i - \boldsymbol{a}_j\|^2 \approx d_0{}^2, \ \forall \ (i,j) \in \mathcal{A}. \tag{3.10}$$

The weights, $\boldsymbol{w} = \sqrt{w_{ij}}$, are introduced in order to give more importance to the nearest links. These weights are defined as:

$$w_{ij} = 1 - \frac{\hat{d}_{ij}^{\mathcal{A}}}{\sum_{(i,j)\in\mathcal{A}} \hat{d}_{ij}^{\mathcal{A}}}, \ \forall \ (i,j) \in \mathcal{A}, \tag{3.11}$$

where $\hat{d}_{ij}^{\mathcal{A}}$ is defined in equation (3.2a). The bigger importance given to the nearby links are due to the fact that both RSS and AoA short-range measurements are more reliable than the long-range measurements.

The RSS errors are considered to as multiplicative [42]. The standard deviation, σ_{ij}, in dB, is constant throughout the distance but the multiplicative factor implies that, for example, when considering a multiplicative factor of 1.4, at a range of 10 meters, a measured range could be of 14 meters, meaning that the RSS error is of 4 meters. When a longer range is considered, for example, 100 meters, the measured range could achieve the 140 meters, having an error of 40 meters, a factor 10 times greater that the previous example. This is the reason why RSS short-range measurements are more reliable. The Fig. 3.1 illustrates this idea.

The AoA errors, as opposed to RSS errors, are referred to as additive [42]. These are not the only source of errors in AoA measurements, multipath also impairs the location estimation. To illustrate this type of error and to give more emphasis to the importance of the closer links, the Fig. 3.2 shows an azimuth angle measurement made between an anchor and two targets located over the same line being one at a short-range and the other at a longer range. The real and the measured angles are denoted by ϕ and $\hat{\phi}$ respectively. It is seen from Fig. 3.2 that the nearest target has better accuracy when the localization process is implemented when compared to the target farther away, despite the fact that the measured azimuth angle is the same.

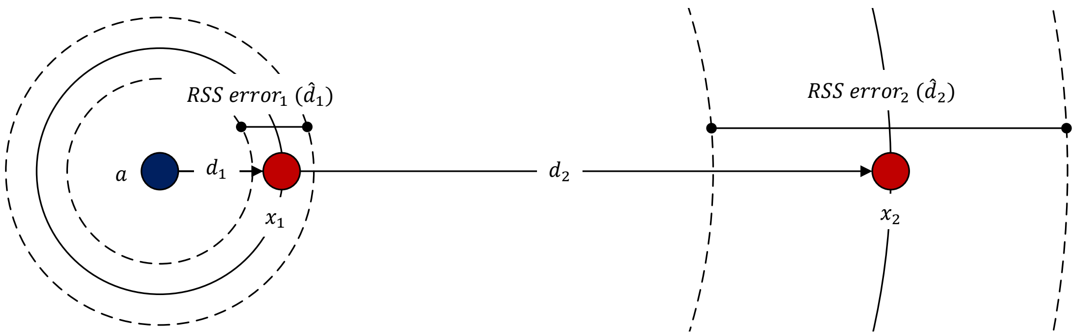

Figure 3.1: RSS measurements: short-range vs long-range

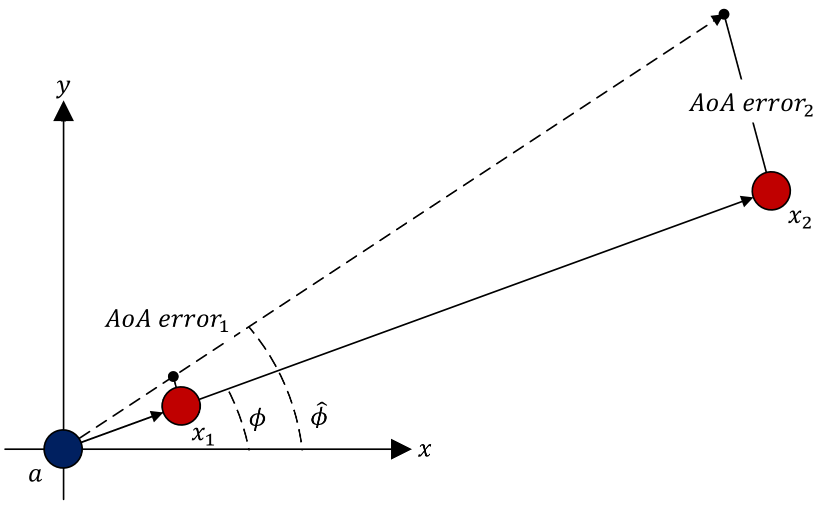

Figure 3.2: AoA measurements: short-range vs long-range

The following step consists in the replacement of $\|\boldsymbol{x}_i - \boldsymbol{a}_j\|$ with $\hat{d}_{ij}^A$ modelled by (3.2a) and according to (3.8), (3.9), (3.10) and (3.11), the below squared range WLS problem is formulated as:

$$\hat{\boldsymbol{x}}_i = \arg\min_{\boldsymbol{x}_i} \sum_{(i,j):(i,j)\in\mathcal{A}} w_{ij}\left(\lambda_{ij}^{\mathcal{A}\,2}\|\boldsymbol{x}_i-\boldsymbol{a}_j\|^2 - {d_0}^2\right)^2 + \sum_{(i,j):(i,j)\in\mathcal{A}} w_{ij}\left(\boldsymbol{c}_{ij}^T\left(\boldsymbol{x}_i-\boldsymbol{a}_j\right)\right)^2$$
$$+ \sum_{(i,j):(i,j)\in\mathcal{A}} w_{ij}\left(\boldsymbol{k}_{ij}^T\left(\boldsymbol{x}_i-\boldsymbol{a}_j\right) - \hat{d}_{ij}^{\mathcal{A}}\cos\left(\alpha_{ij}^{\mathcal{A}}\right)\right)^2. \tag{3.12}$$

The above SR-WLS estimator shares the same properties of the LS problem presented in (3.6) of being non-convex and of not having any closed-form solution. In spite of having these features, it is possible to express (3.12) as a quadratic programming problem resorting to the substitution $\boldsymbol{y}_i = \left[{\boldsymbol{x}_i}^T,\ \|\boldsymbol{x}_i\|^2\right]^T$, thereby making it possible to efficiently compute a global solution for this problem [51]. It is possible to rewrite the problem of (3.12) as:

$$\begin{aligned} &\underset{\boldsymbol{y}_i}{\text{minimize}} && \|\boldsymbol{W}\left(\boldsymbol{A}\boldsymbol{y}_i - \boldsymbol{b}\right)\|^2 \\ &\text{subject to} && {\boldsymbol{y}_i}^T\boldsymbol{D}\boldsymbol{y}_i + 2\boldsymbol{l}^T\boldsymbol{y}_i = 0, \end{aligned} \tag{3.13}$$

where

$$\boldsymbol{W} = \boldsymbol{I}_3 \otimes \operatorname{diag}(\boldsymbol{w}), \qquad \boldsymbol{D} = \begin{bmatrix} \boldsymbol{I}_3 & \boldsymbol{0}_{3\times1} \\ \boldsymbol{0}_{1\times3} & 0 \end{bmatrix}, \qquad \boldsymbol{l} = \begin{bmatrix} \boldsymbol{0}_{3\times1} \\ -\frac{1}{2} \end{bmatrix},$$

$$\boldsymbol{A} = \begin{bmatrix} \vdots & \vdots \\ -2\lambda_{ij}^{\mathcal{A}\,2}{\boldsymbol{a}_j}^T & \lambda_{ij}^{\mathcal{A}\,2} \\ \vdots & \vdots \\ {\boldsymbol{c}_{ij}}^T & 0 \\ \vdots & \vdots \\ {\boldsymbol{k}_{ij}}^T & 0 \\ \vdots & \vdots \end{bmatrix}, \qquad \boldsymbol{b} = \begin{bmatrix} \vdots \\ {d_0}^2 - \lambda_{ij}^{\mathcal{A}\,2}\|\boldsymbol{a}_j\|^2 \\ \vdots \\ {\boldsymbol{c}_{ij}}^T\boldsymbol{a}_j \\ \vdots \\ {\boldsymbol{k}_{ij}}^T\boldsymbol{a}_j + \hat{d}_{ij}^{\mathcal{A}}\cos\left(\alpha_{ij}^{\mathcal{A}}\right) \\ \vdots \end{bmatrix},$$

meaning that $\boldsymbol{A} \in \mathbb{R}^{3|\mathcal{A}|\times4}$, $\boldsymbol{b} \in \mathbb{R}^{3|\mathcal{A}|\times1}$ and $\boldsymbol{W} \in \mathbb{R}^{3|\mathcal{A}|\times3|\mathcal{A}|}$ $\forall(i,j)\in\mathcal{A}$. After having rewritten (3.12) as (3.13) it can be readily shown that not only the objective function but also the constraint in (3.13) have a quadratic form.

When both objective function and constraint are quadratic, the problem is known as a generalized trust region subproblem GTRS [51, 52, 53] and an exact solution can be obtained making use of a bisection procedure [51]. Although non-convex, the problems of this type have the necessaries and the sufficient optimum conditions from which efficient solution methods may be achieved. For the bisection procedure, the optimal solution of (3.13) is given by

$$\hat{\boldsymbol{y}}(\lambda) = \left((\boldsymbol{W}\boldsymbol{A})^T(\boldsymbol{W}\boldsymbol{A}) + \lambda\boldsymbol{D}\right)^{-1}\left((\boldsymbol{W}\boldsymbol{A})^T(\boldsymbol{W}\boldsymbol{b}) - \lambda\boldsymbol{l}\right), \tag{3.14}$$

where λ is the only solution of

$$\varphi(\lambda) = 0, \ \forall \lambda \in I, \tag{3.15}$$

where $\varphi(\lambda)$ and the interval I are defined as follows:

$$\varphi(\lambda) = \hat{\boldsymbol{y}}(\lambda)^T \boldsymbol{D} \hat{\boldsymbol{y}}(\lambda) + 2\boldsymbol{l}^T \hat{\boldsymbol{y}}(\lambda), \tag{3.16}$$

and

$$I = \left(-\frac{1}{\lambda_1 \left(\boldsymbol{D}, (\boldsymbol{WA})^T (\boldsymbol{WA}) \right)}, \ \infty \right), \tag{3.17}$$

where λ_1 is defined as being the highest eigenvalue of $\left(\boldsymbol{D}, (\boldsymbol{WA})^T (\boldsymbol{WA}) \right)$.

The purpose is to use the bisection procedure to obtain λ that satisfies (3.16). After performing this procedure, the coordinates of the estimated target are obtained by replacing the value of λ, obtained by the bisection procedure, in equation (3.14), and the coordinate values are expressed by the first three elements of that equation.

Further considerations were taken into account for this bisection method such as limiting the maximum number of iterations to 30, in order to reduce the computational complexity of the algorithm. Such considerations are explained with more details in Chapter 4. In the remaining text, the algorithm presented in (3.13) will be denoted as "SR-WLS$_1$".

3.3.2 Unknown source transmit power (P_T)

Having an unknown P_T is very common in WSNs, meaning that the P_T is not calibrated. Generally this is done because calibration is not a priority and it is a way to maintain low implementation costs. The lack of knowledge of the P_T corresponds to not knowing L_0 in (3.1a)[45, 54].

Similar to the previous case where P_T is known, the first step is to consider the noise power extremely low. Equations (3.8) stay equal but, due to the fact of not knowing L_0, it is necessary to rewrite (3.7) as:

$$\beta_{ij}^{\mathcal{A}} \| \boldsymbol{x}_i - \boldsymbol{a}_j \| \approx \eta d_0, \ \forall \ (i,j) \in \mathcal{A}, \tag{3.18}$$

where $\beta_{ij}^{\mathcal{A}} = 10^{-\frac{L_{ij}^{\mathcal{A}}}{10\gamma}}$ $\forall (i,j) \in \mathcal{A}$, and $\eta = 10^{-\frac{L_0}{10\gamma}}$ contains an unknown parameter (L_0) which, like the target position, also needs to be estimated. By squaring both sides of (3.18) it is obtained

$$\beta_{ij}^{\mathcal{A}^2} \| \boldsymbol{x}_i - \boldsymbol{a}_j \|^2 \approx \eta^2 {d_0}^2, \ \forall \ (i,j) \in \mathcal{A}. \tag{3.19}$$

The next step consists in the replacement of $\| \boldsymbol{x}_i - \boldsymbol{a}_j \|$ with $\hat{d}_{ij}^{\mathcal{A}}$ in (3.9) which corresponds to rewrite (3.9) as

$$\beta_{ij}^{\mathcal{A}} {\boldsymbol{k}_{ij}}^T \left(\boldsymbol{x}_i - \boldsymbol{a}_j \right) \approx \eta d_0 \cos\left(\alpha_{ij}^{\mathcal{A}} \right), \ \forall \ (i,j) \in \mathcal{A}, \tag{3.20}$$

due to the fact that L_0 is not known. Next, the weights, $\boldsymbol{w} = \sqrt{w_{ij}}$, are re-introduced in order to give greater importance to the nearby links. These weights cannot be equal to the ones presented in the previous subsection because of the lack of knowledge of L_0 in the present case. So, instead of considering the distance measurements ($\hat{d}_{ij}^{\mathcal{A}}$), the path loss measurements ($L_{ij}^{\mathcal{A}}$) are considered for this case by making the weights to be modelled as follows:

$$w_{ij} = 1 - \frac{L_{ij}^{\mathcal{A}}}{\sum_{(i,j)\in\mathcal{A}} L_{ij}^{\mathcal{A}}}, \ \forall\ (i,j) \in \mathcal{A}. \tag{3.21}$$

In accordance with (3.19), (3.8), (3.20) and (3.21), the following step consists in formulating a SR-WLS problem as:

$$\begin{aligned}(\hat{\boldsymbol{x}}_i,\ \hat{\eta}) = \arg\min_{\boldsymbol{x}_i,\eta} & \sum_{(i,j):(i,j)\in\mathcal{A}} w_{ij}\left(\beta_{ij}^{\mathcal{A}\,2}\|\boldsymbol{x}_i - \boldsymbol{a}_j\|^2 - \eta^2 {d_0}^2\right)^2 + \sum_{(i,j):(i,j)\in\mathcal{A}} w_{ij}\left({\boldsymbol{c}_{ij}}^T\left(\boldsymbol{x}_i - \boldsymbol{a}_j\right)\right)^2 \\ & + \sum_{(i,j):(i,j)\in\mathcal{A}} w_{ij}\left(\beta_{ij}^{\mathcal{A}}{\boldsymbol{k}_{ij}}^T\left(\boldsymbol{x}_i - \boldsymbol{a}_j\right) - \eta d_0 \cos\left(\alpha_{ij}^{\mathcal{A}}\right)\right)^2.\end{aligned} \tag{3.22}$$

Next, the SR-WLS problem presented in (3.22) is rewritten as a GTRS making use of the substitution $\boldsymbol{y}_i = \left[{\boldsymbol{x}_i}^T,\ \|\boldsymbol{x}_i\|^2,\ \eta,\ \eta^2\right]^T$

$$\begin{aligned}&\underset{\boldsymbol{y}_i}{\text{minimize}} && \|\boldsymbol{W}\left(\boldsymbol{A}\boldsymbol{y}_i - \boldsymbol{b}\right)\|^2 \\ &\text{subject to} && {\boldsymbol{y}_i}^T\boldsymbol{D}\boldsymbol{y}_i + 2\boldsymbol{l}^T\boldsymbol{y}_i = 0,\end{aligned} \tag{3.23}$$

where

$$\boldsymbol{W} = \boldsymbol{I}_3 \otimes \text{diag}(\boldsymbol{w}), \qquad \boldsymbol{D} = \text{diag}([1,\ 1,\ 1,\ 0,\ 1,\ 0]), \qquad \boldsymbol{l} = \begin{bmatrix}\boldsymbol{0}_{3\times1} \\ -\frac{1}{2} \\ 0 \\ -\frac{1}{2}\end{bmatrix},$$

$$\boldsymbol{A} = \begin{bmatrix} \vdots & \vdots & \vdots & \vdots \\ -2\beta_{ij}^{\mathcal{A}\,2}{\boldsymbol{a}_j}^T & \beta_{ij}^{\mathcal{A}\,2} & 0 & -d_0 \\ \vdots & \vdots & \vdots & \vdots \\ {\boldsymbol{c}_{ij}}^T & 0 & 0 & 0 \\ \vdots & \vdots & \vdots & \vdots \\ \beta_{ij}^{\mathcal{A}}{\boldsymbol{k}_{ij}}^T & 0 & -d_0\cos\left(\alpha_{ij}^{\mathcal{A}}\right) & 0 \\ \vdots & \vdots & \vdots & \vdots \end{bmatrix}, \qquad \boldsymbol{b} = \begin{bmatrix} \vdots \\ -\beta_{ij}^{\mathcal{A}\,2}\|\boldsymbol{a}_j\|^2 \\ \vdots \\ {\boldsymbol{c}_{ij}}^T\boldsymbol{a}_j \\ \vdots \\ \beta_{ij}^{\mathcal{A}}{\boldsymbol{k}_{ij}}^T\boldsymbol{a}_j \\ \vdots \end{bmatrix},$$

meaning that $\boldsymbol{A} \in \mathbb{R}^{3|\mathcal{A}|\times6}$, $\boldsymbol{b} \in \mathbb{R}^{3|\mathcal{A}|\times1}$ and $\boldsymbol{W} \in \mathbb{R}^{3|\mathcal{A}|\times3|\mathcal{A}|}$ $\forall(i,j) \in \mathcal{A}$.

A solution for the approach in (3.23) is obtained through a bisection procedure considering (3.14), (3.15), (3.16) and (3.17), presented in the previous subsection, solving efficiently the localization problem formulated in (3.6), for this case, when P_T is unknown.

However, the accuracy of the target location can be improved. By exploiting the ML estimate of L_0, resorting to the previous target location estimate, modelled as follows:

$$\hat{L}_0 = \frac{\sum_{(i,j)\in\mathcal{A}}\left(L_{ij}^{\mathcal{A}} - 10\gamma\log_{10}\left(\frac{\|\hat{\boldsymbol{x}}_i' - \boldsymbol{a}_j\|}{d_0}\right)\right)}{|\mathcal{A}|}, \ \forall\ (i,j)\in\mathcal{A}, \tag{3.24}$$

it has been seen in the simulations, that with this estimation of L_0 in (3.24), values very close to the true value of L_0 are obtained. Thus, advantage of this estimate of L_0 is taken to compute $\hat{d}_{ij}^{\mathcal{A}}$ and $\hat{\lambda}_{ij}^{\mathcal{A}}$ to solve another SR-WLS problem (3.12) as if P_T was known, as presented in the previous subsection.

The summary of a three-step the procedure is shown as follows:

1. Solve (3.23) to obtain an initial target location denoted as $\boldsymbol{x}_i'$;

2. Compute the ML estimate of L_0, $\hat{L}_0$, with (3.24);

3. Calculate $\hat{d}_{ij}^{\mathcal{A}}$ and $\hat{\lambda}_{ij}^{\mathcal{A}}$, using $\hat{L}_0$, to solve the SR-WLS in (3.13).

This three-step procedure is denoted as "SR-WLS$_2$" in the remaining text.

3.4 Cooperative Localization

For a cooperative localization scenario in a WSN, comprising targets and anchors, where a target is able to communicate with any other sensor in its communication range (R), the targets location are estimated simultaneously. This communication range should be as small as possible particularly in networks with lack of energy resources to promote the sensors lifespan. By limiting this range, there may be targets on the network that are not able to communicate with anchors directly, and due to this fact, node cooperation becomes fundamental to make possible to locate all targets [55, 56].

Due to the fact of a target being capable to communicate with any other sensor within its communication range, in this scenario type, targets are not passive nodes. Instead, they are considered pseudo-anchors. Contrary to the non-cooperative location scenario, the set $\mathcal{B}$ is not empty, then it resorts to (3.1a), (3.2a), (3.3a) and (3.4a) to calculate, respectively, the path loss, the approximated distance, the azimuth and the elevation angles for the set $\mathcal{A}$ and, for set $\mathcal{B}$ is made use of (3.1b), (3.2b), (3.3b) and (3.4b).

To solve the localization problem presented in (3.6), for this cooperative scenario, a convex estimator is used, obtaining the exact solution through interior-point algorithms. This estimator and the method are explained with more detail in the following subsections [57].

3.4.1 Known source transmit power (P_T)

Similarly to the non-cooperative scenario, the first step, when the P_T is known, is to consider sufficiently low noise resulting in:

$$\lambda_{ik}^{\mathcal{B}} \|\boldsymbol{x}_i - \boldsymbol{x}_k\| \approx d_0,\ \forall\ (i,k) \in \mathcal{B}, \tag{3.25}$$

$$\boldsymbol{c}_{ik}{}^T (\boldsymbol{x}_i - \boldsymbol{x}_k) \approx 0,\ \forall\ (i,k) \in \mathcal{B}, \tag{3.26}$$

$$\boldsymbol{k}_{ij}{}^T \left(\boldsymbol{x}_i - \boldsymbol{a}_j\right)\left(\boldsymbol{x}_i - \boldsymbol{a}_j\right)^T \boldsymbol{k}_{ij} \approx \|\boldsymbol{x}_i - \boldsymbol{a}_j\|^2 \cos^2\left(\alpha_{ij}^{\mathcal{A}}\right),\ \forall\ (i,j) \in \mathcal{A}, \tag{3.27}$$

$$\boldsymbol{k}_{ik}{}^T (\boldsymbol{x}_i - \boldsymbol{x}_k)(\boldsymbol{x}_i - \boldsymbol{x}_k)^T \boldsymbol{k}_{ik} \approx \|\boldsymbol{x}_i - \boldsymbol{x}_k\|^2 \cos^2\left(\alpha_{ik}^{\mathcal{B}}\right),\ \forall\ (i,k) \in \mathcal{B}, \tag{3.28}$$

where $\lambda_{ik}^{\mathcal{B}} = 10^{\frac{L_0 - L_{ik}^{\mathcal{B}}}{10\gamma}}$, $\boldsymbol{c}_{ik} = [-\sin\left(\phi_{ik}^{\mathcal{B}}\right),\ \cos\left(\phi_{ik}^{\mathcal{B}}\right),\ 0]^T$ and $\boldsymbol{k}_{ik} = [0,\ 0,\ 1]^T\ \forall (i,k) \in \mathcal{B}$. Considering the noise power rather small, the equations (3.1a) and (3.3a) result in equations (3.7) and (3.8) that are also used in this scenario.

The next step consists in re-arranging the above equations, according to the LS principle, to obtain the localization problem. Squaring equations (3.7) and (3.25) and making use of (3.8), (3.9), (3.26) and (3.28), the estimation of the targets location is obtained by minimizing the following objective function:

$$\begin{aligned}
\hat{\boldsymbol{x}} = \arg\min_{\boldsymbol{x}} & \sum_{(i,j):(i,j)\in\mathcal{A}} \left(\lambda_{ij}^{\mathcal{A}\,2} \|\boldsymbol{x}_i - \boldsymbol{a}_j\|^2 - d_0{}^2\right)^2 + \sum_{(i,j):(i,j)\in\mathcal{A}} \left(\boldsymbol{c}_{ij}{}^T \left(\boldsymbol{x}_i - \boldsymbol{a}_j\right)\right)^2 \\
& + \sum_{(i,j):(i,j)\in\mathcal{A}} \left(\boldsymbol{k}_{ij}{}^T \left(\boldsymbol{x}_i - \boldsymbol{a}_j\right)\left(\boldsymbol{x}_i - \boldsymbol{a}_j\right)^T \boldsymbol{k}_{ij} - \|\boldsymbol{x}_i - \boldsymbol{a}_j\|^2 \cos^2\left(\alpha_{ij}^{\mathcal{A}}\right)\right)^2 \\
& + \sum_{(i,k):(i,k)\in\mathcal{B}} \left(\lambda_{ik}^{\mathcal{B}\,2} \|\boldsymbol{x}_i - \boldsymbol{x}_k\|^2 - d_0{}^2\right)^2 + \sum_{(i,k):(i,k)\in\mathcal{B}} \left(\boldsymbol{c}_{ik}{}^T (\boldsymbol{x}_i - \boldsymbol{x}_k)\right)^2 \\
& + \sum_{(i,k):(i,k)\in\mathcal{B}} \left(\boldsymbol{k}_{ik}{}^T (\boldsymbol{x}_i - \boldsymbol{x}_k)(\boldsymbol{x}_i - \boldsymbol{x}_k)^T \boldsymbol{k}_{ik} - \|\boldsymbol{x}_i - \boldsymbol{x}_k\|^2 \cos^2\left(\alpha_{ik}^{\mathcal{B}}\right)\right)^2.
\end{aligned} \tag{3.29}$$

Although the optimization problem presented in (3.29) shares the exact same problems of the LS problem presented in (3.6) and the SR-WLS presented in (3.12) and (3.22), of being non-convex and of not having any closed-form solution, the following step is the conversion of this problem to a SDP problem.

It is very common to stack up all the unknown targets location in one only matrix $\boldsymbol{Y} = [\boldsymbol{x}_1, \ldots, \boldsymbol{x}_M]$ $\left(\boldsymbol{Y} \in \mathbb{R}^{3\times M}\right)$, as in [23, 24, 27, 28]. However, due to some mathematical conflicts, this approach is not suitable to solve (3.29). The conflict is related with the vector outer product, presented in sums of two parcels of the above equation, with respect to elevation angles. To overcome this problem, instead of one big matrix, a vector to stack all the unknown targets as $\boldsymbol{x} = \left[\boldsymbol{x}_1{}^T, \ldots, \boldsymbol{x}_M{}^T\right]^T$ $\left(\boldsymbol{x} \in \mathbb{R}^{3M\times 1}\right)$ is used.

Resorting to an auxiliary variable $\boldsymbol{X} = \boldsymbol{x}\boldsymbol{x}^T$ $\left(\boldsymbol{X} \in \mathbb{R}^{3M \times 3M}\right)$ and to an auxiliary vector $\boldsymbol{z} = \left[\boldsymbol{z}_{ij}^{\mathcal{A}}, \boldsymbol{g}_{ij}^{\mathcal{A}}, \boldsymbol{p}_{ij}^{\mathcal{A}}, \boldsymbol{z}_{ik}^{\mathcal{B}}, \boldsymbol{g}_{ik}^{\mathcal{B}}, \boldsymbol{p}_{ik}^{\mathcal{B}}\right]^T$ $\left(\boldsymbol{z} \in \mathbb{R}^{3(|\mathcal{A}|+|\mathcal{B}|\times 1)}\right)$, the problem presented in (3.29) may be rewritten as:

$$\begin{aligned}
&\underset{\boldsymbol{x},\boldsymbol{X},\boldsymbol{z}}{\text{minimize}} \quad \|\boldsymbol{z}\|^2 \\
&\text{subject to} \\
&\boldsymbol{z}_{ij}^{\mathcal{A}} = \lambda_{ij}^{\mathcal{A}\,2}\left(\text{tr}\left(\boldsymbol{E}_i{}^T\boldsymbol{X}\boldsymbol{E}_i\right) - 2\boldsymbol{a}_j{}^T\boldsymbol{E}_i{}^T\boldsymbol{x} + \|\boldsymbol{a}_j\|^2\right) - d_0{}^2, &(3.30a)\\
&\boldsymbol{g}_{ij}^{\mathcal{A}} = \boldsymbol{c}_{ij}{}^T\left(\boldsymbol{E}_i{}^T\boldsymbol{x} - \boldsymbol{a}_j\right), &(3.30b)\\
&\boldsymbol{p}_{ij}^{\mathcal{A}} = \boldsymbol{k}_{ij}{}^T\left(\boldsymbol{E}_i{}^T\boldsymbol{X}\boldsymbol{E}_i - 2\boldsymbol{E}_i{}^T\boldsymbol{x}\boldsymbol{a}_j{}^T + \boldsymbol{a}_j\boldsymbol{a}_j{}^T\right)\boldsymbol{k}_{ij}\\
&\quad - \left(\text{tr}\left(\boldsymbol{E}_i{}^T\boldsymbol{X}\boldsymbol{E}_i\right) - 2\boldsymbol{a}_j{}^T\boldsymbol{E}_i{}^T\boldsymbol{x} + \|\boldsymbol{a}_j\|^2\right)\cos^2\left(\alpha_{ij}^{\mathcal{A}}\right), &(3.30c)\\
&\boldsymbol{z}_{ik}^{\mathcal{B}} = \lambda_{ik}^{\mathcal{B}\,2}\left(\text{tr}\left(\boldsymbol{E}_i{}^T\boldsymbol{X}\boldsymbol{E}_i\right) - 2\text{tr}\left(\boldsymbol{E}_i{}^T\boldsymbol{X}\boldsymbol{E}_k\right) + \text{tr}\left(\boldsymbol{E}_k{}^T\boldsymbol{X}\boldsymbol{E}_k\right)\right) - d_0{}^2, &(3.30d)\\
&\boldsymbol{g}_{ik}^{\mathcal{B}} = \boldsymbol{c}_{ik}{}^T\left(\boldsymbol{E}_i{}^T\boldsymbol{x} - \boldsymbol{E}_k{}^T\boldsymbol{x}\right), &(3.30e)\\
&\boldsymbol{p}_{ik}^{\mathcal{B}} = \boldsymbol{k}_{ik}{}^T\left(\boldsymbol{E}_i{}^T\boldsymbol{X}\boldsymbol{E}_i - 2\boldsymbol{E}_i{}^T\boldsymbol{X}\boldsymbol{E}_k + \boldsymbol{E}_k{}^T\boldsymbol{X}\boldsymbol{E}_k\right)\boldsymbol{k}_{ik}\\
&\quad - \left(\text{tr}\left(\boldsymbol{E}_i{}^T\boldsymbol{X}\boldsymbol{E}_i\right) - 2\text{tr}\left(\boldsymbol{E}_i{}^T\boldsymbol{X}\boldsymbol{E}_k\right) + \text{tr}\left(\boldsymbol{E}_k{}^T\boldsymbol{X}\boldsymbol{E}_k\right)\right)\cos^2\left(\alpha_{ik}^{\mathcal{B}}\right), &(3.30f)\\
&\boldsymbol{X} = \boldsymbol{x}\boldsymbol{x}^T, &(3.30g)
\end{aligned}$$

$\forall (i,j) \in \mathcal{A}$ and $(i,k) \in \mathcal{B}$.

The semidefinite and the second-order cone relaxations of the form, respectively, $\boldsymbol{X} \succeq \boldsymbol{x}\boldsymbol{x}^T$ and $\|\boldsymbol{z}\|^2 \leq t$, where t is an epigraph variable, jointly, and based on the problem mentioned above, constitute the next convex optimization problem:

$$\begin{aligned}
&\underset{\boldsymbol{x},\boldsymbol{X},\boldsymbol{z},t}{\text{minimize}} && t \\
&\text{subject to} && \text{(3.30a)-(3.30f)},\\
& && \left\|\begin{bmatrix} 2\boldsymbol{z}, \\ t-1 \end{bmatrix}\right\| \leq t+1,\\
& && \begin{bmatrix} \boldsymbol{X} & \boldsymbol{x} \\ \boldsymbol{x}^T & 1 \end{bmatrix} \succeq \boldsymbol{0}_{3M+1}.
\end{aligned} \tag{3.31}$$

The above problem (3.31) is a convex optimization problem known as SDP. It is not a pure SDP, more precisely it is a mixed SDP/SOCP problem and it can be solved using CVX, a package for specifying and solving convex programs [58, 59]. The Schur complement, presented in [57, 60], was used to rewrite (3.30g) as a semidefinite cone constraint. The algorithm presented in (3.31) will be denoted as "SDP_1" in the remaining text.

3.4.2 Unknown source transmit power (P_T)

Starting with sufficiently small noise, the equations (3.18), (3.8) and (3.26) and, (3.9) and (3.28), corresponding respectively to the path loss, azimuth and elevation measures, remain the same and are used for this scenario. The path loss model for the set $\mathcal{B}$ in a cooperative scenario can be approximated as follows:

$$\beta_{ik}^{\mathcal{B}}\|\boldsymbol{x}_i - \boldsymbol{x}_k\| \approx \eta d_0, \ \forall \ (i,k) \in \mathcal{B}, \tag{3.32}$$

where $\beta_{ik}^{\mathcal{B}} = 10^{-\frac{L_{ik}^{\mathcal{B}}}{10\gamma}}$ $\forall (i,k) \in \mathcal{B}$ and, as previously seen on the text, $\eta = 10^{-\frac{L_0}{10\gamma}}$ which contains the unknown parameter (L_0) corresponding to the lack of knowledge of P_T. This unknown parameter, as the target location, also needs to be estimated.

Following, and according to the LS principle, once again, the above equations needs to be re-arranged in a manner to obtain the localization problem. Squaring equations (3.18) and (3.32) and using the equations (3.8), (3.9), (3.26) and (3.28), the problem below can be obtained to estimate the targets location.

$$\begin{aligned}(\hat{\boldsymbol{x}},\ \hat{\eta}) = \arg\min_{\boldsymbol{x},\eta} & \sum_{(i,j):(i,j)\in\mathcal{A}} \left(\beta_{ij}^{\mathcal{A}\,2}\|\boldsymbol{x}_i - \boldsymbol{a}_j\|^2 - \eta^2 {d_0}^2\right)^2 + \sum_{(i,j):(i,j)\in\mathcal{A}} \left({\boldsymbol{c}_{ij}}^T\left(\boldsymbol{x}_i - \boldsymbol{a}_j\right)\right)^2 \\ &+ \sum_{(i,j):(i,j)\in\mathcal{A}} \left({\boldsymbol{k}_{ij}}^T\left(\boldsymbol{x}_i - \boldsymbol{a}_j\right)\left(\boldsymbol{x}_i - \boldsymbol{a}_j\right)^T \boldsymbol{k}_{ij} - \|\boldsymbol{x}_i - \boldsymbol{a}_j\|^2 \cos^2\left(\alpha_{ij}^{\mathcal{A}}\right)\right)^2 \\ &+ \sum_{(i,k):(i,k)\in\mathcal{B}} \left(\beta_{ik}^{\mathcal{B}\,2}\|\boldsymbol{x}_i - \boldsymbol{x}_k\|^2 - \eta^2 {d_0}^2\right)^2 + \sum_{(i,k):(i,k)\in\mathcal{B}} \left({\boldsymbol{c}_{ik}}^T\left(\boldsymbol{x}_i - \boldsymbol{x}_k\right)\right)^2 \\ &+ \sum_{(i,k):(i,k)\in\mathcal{B}} \left({\boldsymbol{k}_{ik}}^T\left(\boldsymbol{x}_i - \boldsymbol{x}_k\right)\left(\boldsymbol{x}_i - \boldsymbol{x}_k\right)^T \boldsymbol{k}_{ik} - \|\boldsymbol{x}_i - \boldsymbol{x}_k\|^2 \cos^2\left(\alpha_{ik}^{\mathcal{B}}\right)\right)^2. \end{aligned} \tag{3.33}$$

The next step is identical to the one made for the cooperative case with known P_T; the differences here are that, instead of $\lambda_{ij}^{\mathcal{A}}$ and $\lambda_{ik}^{\mathcal{B}}$ it has $\beta_{ij}^{\mathcal{A}}$ and $\beta_{ik}^{\mathcal{B}}$ and here, a new variable (ρ) is introduced. The problem in (3.33) is rewritten as:

$$\underset{\boldsymbol{x},\rho,\boldsymbol{X},\boldsymbol{z}}{\text{minimize}} \quad \|\boldsymbol{z}\|^2$$

subject to

$$\boldsymbol{z}_{ij}^{\mathcal{A}} = \beta_{ij}^{\mathcal{A}\,2}\left(\text{tr}\left({\boldsymbol{E}_i}^T\boldsymbol{X}\boldsymbol{E}_i\right) - 2{\boldsymbol{a}_j}^T{\boldsymbol{E}_i}^T\boldsymbol{x} + \|\boldsymbol{a}_j\|^2\right) - \rho^2 {d_0}^2, \tag{3.34a}$$

$$\boldsymbol{g}_{ij}^{\mathcal{A}} = {\boldsymbol{c}_{ij}}^T\left({\boldsymbol{E}_i}^T\boldsymbol{x} - \boldsymbol{a}_j\right), \tag{3.34b}$$

$$\begin{aligned}\boldsymbol{p}_{ij}^{\mathcal{A}} &= {\boldsymbol{k}_{ij}}^T\left({\boldsymbol{E}_i}^T\boldsymbol{X}\boldsymbol{E}_i - 2{\boldsymbol{E}_i}^T\boldsymbol{x}{\boldsymbol{a}_j}^T + \boldsymbol{a}_j{\boldsymbol{a}_j}^T\right)\boldsymbol{k}_{ij} \\ &- \left(\text{tr}\left({\boldsymbol{E}_i}^T\boldsymbol{X}\boldsymbol{E}_i\right) - 2{\boldsymbol{a}_j}^T{\boldsymbol{E}_i}^T\boldsymbol{x} + \|\boldsymbol{a}_j\|^2\right)\cos^2\left(\alpha_{ij}^{\mathcal{A}}\right),\end{aligned} \tag{3.34c}$$

$$\boldsymbol{z}_{ik}^{\mathcal{B}} = \beta_{ik}^{\mathcal{B}\,2}\left(\text{tr}\left({\boldsymbol{E}_i}^T\boldsymbol{X}\boldsymbol{E}_i\right) - 2\text{tr}\left({\boldsymbol{E}_i}^T\boldsymbol{X}\boldsymbol{E}_k\right) + \text{tr}\left({\boldsymbol{E}_k}^T\boldsymbol{X}\boldsymbol{E}_k\right)\right) - \rho^2 {d_0}^2, \tag{3.34d}$$

$$\boldsymbol{g}_{ik}^{\mathcal{B}} = {\boldsymbol{c}_{ik}}^T\left({\boldsymbol{E}_i}^T\boldsymbol{x} - {\boldsymbol{E}_k}^T\boldsymbol{x}\right), \tag{3.34e}$$

$$\begin{aligned}\boldsymbol{p}_{ik}^{\mathcal{B}} &= {\boldsymbol{k}_{ik}}^T\left({\boldsymbol{E}_i}^T\boldsymbol{X}\boldsymbol{E}_i - 2{\boldsymbol{E}_i}^T\boldsymbol{X}\boldsymbol{E}_k + {\boldsymbol{E}_k}^T\boldsymbol{X}\boldsymbol{E}_k\right)\boldsymbol{k}_{ik} \\ &- \left(\text{tr}\left({\boldsymbol{E}_i}^T\boldsymbol{X}\boldsymbol{E}_i\right) - 2\text{tr}\left({\boldsymbol{E}_i}^T\boldsymbol{X}\boldsymbol{E}_k\right) + \text{tr}\left({\boldsymbol{E}_k}^T\boldsymbol{X}\boldsymbol{E}_k\right)\right)\cos^2\left(\alpha_{ik}^{\mathcal{B}}\right),\end{aligned} \tag{3.34f}$$

$$\boldsymbol{X} = \boldsymbol{x}\boldsymbol{x}^T, \tag{3.34g}$$

$\forall(i,j) \in \mathcal{A}$ and $(i,k) \in \mathcal{B}$ and where ρ is equal to η^2. The necessity of re-writing this variable was due to a mathematical conflict. If η^2 was used, the problem was not convex and could not be solved. This substitution was made without loss of generality.

Next, the semidefinite and the second-order cone relaxations of the form $\boldsymbol{X} \succeq \boldsymbol{x}\boldsymbol{x}^T$ and $\|\boldsymbol{z}\|^2 \leq t$, are used along with equations (3.34a-3.34f) to obtain the following SDP estimator:

$$\begin{aligned}
\underset{\boldsymbol{x},\rho,\boldsymbol{X},\boldsymbol{z},t}{\text{minimize}} \quad & t \\
\text{subject to} \quad & \text{(3.34a)-(3.34f)}, \\
& \left\| \begin{bmatrix} 2\boldsymbol{z}, \\ t-1 \end{bmatrix} \right\| \leq t+1, \\
& \begin{bmatrix} \boldsymbol{X} & \boldsymbol{x} \\ \boldsymbol{x}^T & 1 \end{bmatrix} \succeq \boldsymbol{0}_{3M+1}.
\end{aligned} \tag{3.35}$$

A solution for the above SDP estimator is obtained using the CVX package [58, 59] in the Matlab software. Although the estimator, presented in (3.35), solves the localization problem efficiently, the accuracy of the target location can be improved through the exploitation of ML estimation of L_0, corresponding to the lack of knowledge of P_T. Taking advantage of the previous targets location estimation, the ML estimator can be modelled as follows:

$$\hat{L}_0 = \frac{\sum_{(i,j):(i,j)\in\mathcal{A}} \left(L_{ij}^{\mathcal{A}} - 10\gamma \log_{10}\left(\frac{\|\boldsymbol{E}_i{}^T\hat{\boldsymbol{x}}' - \boldsymbol{a}_j\|}{d_0} \right) \right) + \sum_{(i,k):(i,k)\in\mathcal{B}} \left(L_{ik}^{\mathcal{B}} - 10\gamma \log_{10}\left(\frac{\|\boldsymbol{E}_i{}^T\hat{\boldsymbol{x}}' - \boldsymbol{E}_k{}^T\hat{\boldsymbol{x}}'\|}{d_0} \right) \right)}{|\mathcal{A}| + |\mathcal{B}|},$$
$$\forall\ (i,j) \in \mathcal{A} \text{ and } (i,k) \in \mathcal{B} \tag{3.36}$$

It was verified, in the simulations, that the values obtained with this estimation are close to the true value of L_0. So, this estimation is used to perform another SDP problem as the P_T was known.

As it was done for the case of unknown P_T in the non-cooperative scenario, next, a summary of the proposed model with a three-step procedure for the case of unknown P_T in the cooperative scenario is shown:

1. Solve (3.35) to obtain a initial estimation of all the targets location in the network denoted as $\hat{\boldsymbol{x}}'$;

2. Compute the ML estimate of L_0, $\hat{L}_0$, resorting to (3.36);

3. Calculate $\hat{\lambda}_{ij}^{\mathcal{A}}$ and $\hat{\lambda}_{ik}^{\mathcal{B}}$, using $\hat{L}_0$, to solve the SDP problem in (3.31).

This three-step procedure is denoted as "SDP_2" in the following. With this procedure, the hybrid localization system implementation is concluded for all the studied cases.

Chapter 4

Performance Results

4.1 Introduction

This chapter has the main objective of presenting the implementation of the proposed hybrid localization model. It begins with the complexity analysis of the considered algorithms in Section 4.2, which have been addressed in the previous chapter. It is followed by the simulations results, in Section 4.3, which is divided in two subsections corresponding to the non-cooperative and the cooperative scenarios where the results are discussed.

4.2 Complexity Analysis

Besides the performance of a given algorithm, a very important factor is its computational complexity. This is one of the key features that may define the potential applicability of an algorithm.

To analyse the complexities of the formulated approaches in this work, the worst computational complexity case of a mixed SDP/SOCP is considered, and is given by:

$$\mathcal{O}\left(\sqrt{L}\left(m\sum_{i=1}^{N_{sd}} {n_i^{sd}}^3 + m^2\sum_{i=1}^{N_{sd}} {n_i^{sd}}^2 + m^2\sum_{i=1}^{N_{soc}} n_i^{soc} + \sum_{i=1}^{N_{soc}} {n_i^{soc}}^2 + m^3\right)\right), \tag{4.1}$$

where L is the iteration complexity of the considered algorithm, m is the number of equality constraints, n_i^{sd} and n_i^{soc} are the dimensions of the i-th semidefinite cone and of the second-order cone, respectively, and N_i^{sd} and N_i^{soc} are the number of constraints of, respectively, the semidefinite and the second-order cones [61].

In order to investigate the worst asymptotically case possible, only the dominating elements are presented, which are expressed as functions of N and M. Despite of the limited range (R), derived by energy restrictions, for example, it is assumed that the network is fully connected, being the total number of connections given by:

$$\mathcal{C} = |\,\mathcal{A}\,| + |\,\mathcal{B}\,|,$$

where $|\,\mathcal{A}\,| = MN$ and $|\,\mathcal{B}\,| = \frac{M(M-1)}{2}$. Knowing that in a non-cooperative localization scheme, a target is located at a time, it can be assumed that for that case, $M = 1$.

The maximum number of iterations considered in the bisection procedure, used to solve the non-cooperative localization problem in section 3.3, are denoted as K_{max}. Next, in table 4.1, a brief overview of the considered algorithms with their worst computational complexity cases is provided.

Table 4.1: Complexity Analysis Summary

Algorithm	Description	Complexity
SR-WLS_1	Proposed SR-WLS estimator described in Sec. 3.3.1	$\mathcal{O}(K_{max}N)$
SR-WLS_2	Proposed SR-WLS estimator described in Sec. 3.3.2	$2\mathcal{O}(K_{max}N)$
SDP_1	Proposed SDP estimator described in Sec. 3.4.1	$\mathcal{O}\left(\sqrt{3M}\left(81M^4\left(N+\frac{M}{2}\right)^2\right)\right)$
SDP_2	Proposed SDP estimator described in Sec. 3.4.2	$2\mathcal{O}\left(\sqrt{3M}\left(81M^4\left(N+\frac{M}{2}\right)^2\right)\right)$

From Table 4.1 it can be concluded that the entire computational complexity of the proposed algorithms depends primarily on the number of sensors existing in the network. Another fact which can be observed from the table, is that the complexity of the considered approaches for cooperative localization is significantly higher when compared with the complexity of those approaches considered for non-cooperative localization. This higher complexity was expected since the cooperative localization problem has more constraints, and in particular, the limited range (R), which make almost impossible to some targets be able to communicate with any anchors in the network.

4.3 Simulations Results

In order to evaluate and validate the proposed algorithms, simulations have been made resorting to MATLAB software. In order to have a term of comparison, and to demonstrate the advantages of a hybrid localization system, the considered approaches with known P_T were also employed using only RSS measurements, denoted as SR-WLS_{RSS} and SDP_{RSS} for the respective scenarios. For the cooperative scenario, as mentioned before in the text, the package CVX [58, 59] with the solver SeDuMi [62] was used.

To perform the simulations, a random deployment of all nodes, comprehending targets and anchors, was made within a box with length of $B = 15$ meters long, in each Monte Carlo (M_c) run. A random deployment was considered for a more realistic scenario as stated in page 5.

To simulate the radio measurements, encompassing the AoA and the RSS measures, equations (3.1), (3.3) and (3.4) were used. For these equations, the considered reference distance is $d_0 = 1$ meter with a reference path loss of $L_0 = 40$ dB. The standard deviations for measurement errors were set to $\sigma_n = 6$ dB, $\sigma_m = 10$ degrees and $\sigma_v = 10$ degrees, and the PLE value for each connection between any two sensors was selected from a uniform distribution being a random value in the interval $\gamma \in [2.2, 2.8]$. For the approaches considered, instead of using a random value of PLE in the interval mentioned above, a fixed mean value of $\gamma = 2.5$ was used to calculate the approximated distances ($d_{ij}^{\mathcal{A}}$) used in the non-cooperative scenario to perform the weights, and to calculate $\lambda_{ij}^{\mathcal{A}}$, $\beta_{ij}^{\mathcal{A}}$, $\lambda_{ik}^{\mathcal{B}}$ and $\beta_{ik}^{\mathcal{B}}$ in the appropriate scenarios when there is sufficiently small noise.

It is also worth mentioning that for each case of known and unknown P_T in both scenario types, cooperative and non-cooperative, the same generated radio measurements with the same random deployment were employed in order to make the best comparison possible between the results for known and unknown P_T.

4.3.1 Non-Cooperative Localization Results

Knowing that in a non-cooperative WSN, targets only communicate with anchors and that only one target is located at a time. For the simulations performed in this scenario, it was assumed that $M = 1$, and the targets were assumed to be capable of communicate with any anchor in the network without any communication range restriction. The radio measurements were performed exclusively by anchors. The maximum number of iterations used for the bisection method was set to $K_{max} = 30$ and the number of Monte Carlo runs considered was $M_c = 50000$.

To evaluate the algorithms performance in this non-cooperative case, the metric used was the root mean square error (RMSE) which is a very common error metric used for numerical predictions, defined as follows:

$$RMSE = \sqrt{\sum_{i=1}^{M_c} \frac{||x_i - \hat{x}_i||^2}{M_c}},$$

where $\hat{x}_i$ represents the estimated location of the target x_i from the i-th M_c run.

Fig. 4.1 presents the simulation results for the SR-WLS approaches considered for this scenario illustrating the RMSE versus N comparison. As expected, increasing the number of anchors in the network leads to a better estimation accuracy since there is more reliable information available. Also, it can be observed, from this figure, that the hybrid localization system with known and unknown P_T, "SR-WLS$_1$" and "SR-WLS$_2$", respectively, outperforms a system using just RSS, "SR-WLS$_{RSS}$".

For the proposed algorithms, it can be seen that the gap between them is decreasing with the increasing number of anchors (N). This was also expected due to the fact that more and better information is available making possible to estimate L_0, for "SR-WLS$_2$",

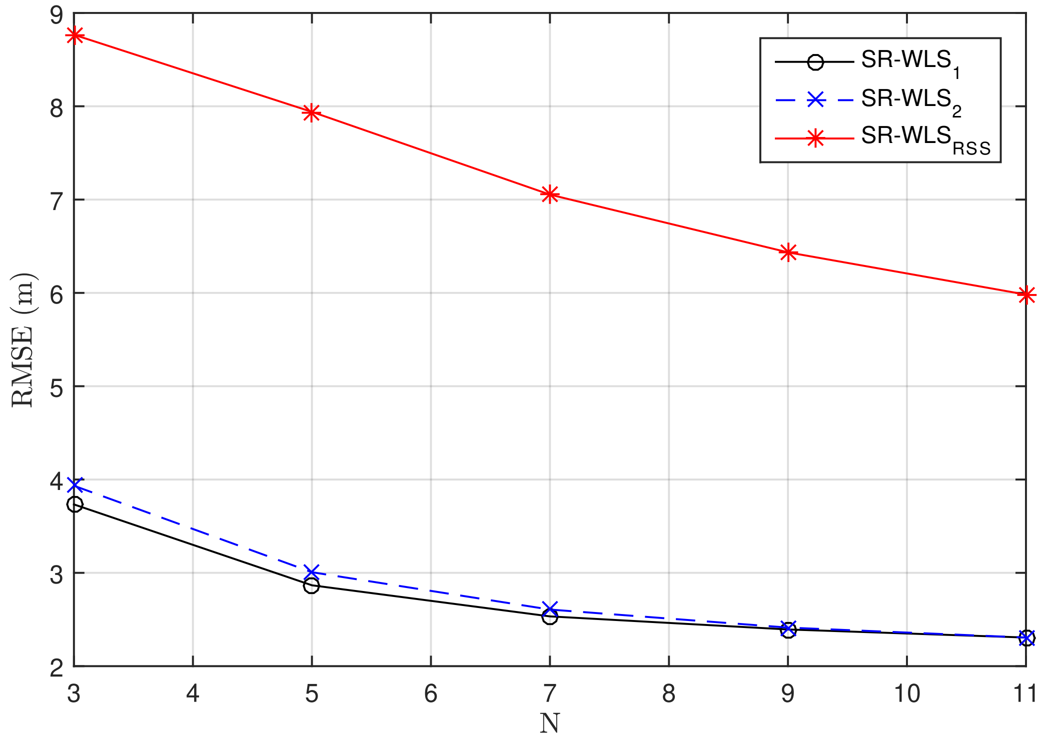

Figure 4.1: RMSE versus N comparison

with a shorter margin of error. So, as the value of L_0 is closer to it's true value, the margin from the implemented approaches trends to reduce.

Having analysed the performance of the considered algorithms, an analyses on how the measurement errors could affect their estimation accuracy was made. For such, the standard deviation of the measurement error studied was varied, while the others remained unchanged, for $N = 4$. Comparing the next three Figs. (4.2), (4.3) and (4.4) where the quality of the measurements of RSS, azimuth and elevation angles, respectively, were represented, it can be observed that with the decrease of the quality of these measurements, the estimation accuracy of the considered approaches worsens.

In Fig. 4.2 it can be seen that the error associated to the RSS measurements affects, significantly, the proposed approaches. The standard deviation of the RSS error ($\sigma_{n_{ij}}$), was varied from one to six decibels, while the standard deviations corresponding to the angles errors, both azimuth and elevation, were maintained at ten degrees.

When compared both considered approaches with "SR-WLS$_{RSS}$", it is verified that this latter continues to show a worse performance than the others.

In Fig. 4.3, it is seen that the error associated to the azimuth angle measures affects, in a smaller scale, the considered approaches. The "SR-WLS$_{RSS}$" performance does not vary because only RSS measures are considered, so the angles errors do not affect this approach. Here, the standard deviation of the azimuth angle error ($\sigma_{m_{ij}}$) was varied from

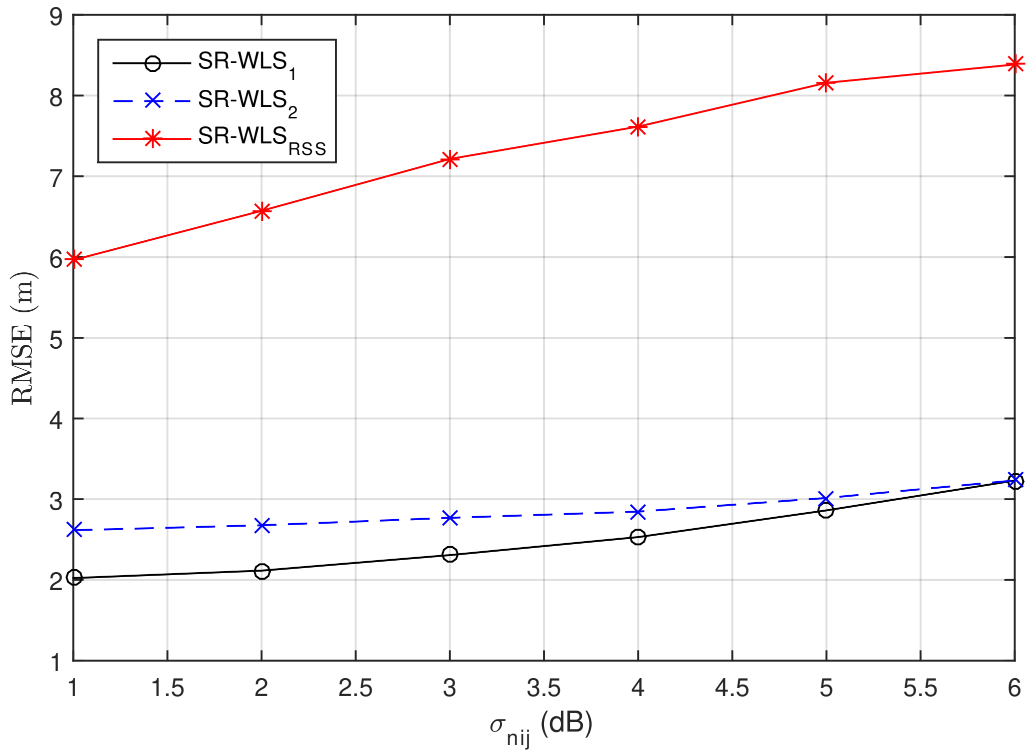

Figure 4.2: RMSE versus $\sigma_{n_{ij}}$ comparison

two to ten degrees while the standard deviation of RSS error was fixed at six decibels and the standard deviation associated to the elevation angle was maintained at ten degrees.

The Fig. 4.4 shows how the elevation angle error maintains the performance of the considered approaches. In this simulation, the standard deviation coupled to the elevation angle error ($\sigma_{v_{ij}}$) was varied from two to ten degrees and the standard deviation from RSS measurement error was kept at six decibels and the other one, associated to the azimuth angle error, at ten degrees. As presented in the previous simulation, in Fig. (4.3) for azimuth angle, this error also does not affect the performance of "SR-WLS$_{RSS}$" since this algorithm does not take into account any type of angle measurements.

Comparing the simulation results of the three simulations, Figs. (4.2), (4.3) and (4.4), it can be concluded that the noise which most affects the performance of the considered approaches is the one associated to the RSS measurements. The noise which has the lowest impact on their performance is the one associated to the elevation angle measurements. It can also be concluded that the considered approaches have a superior performance in comparison to a system that only uses one type of measurements, validating the fact that combining two types of measures improves substantially the localization process.

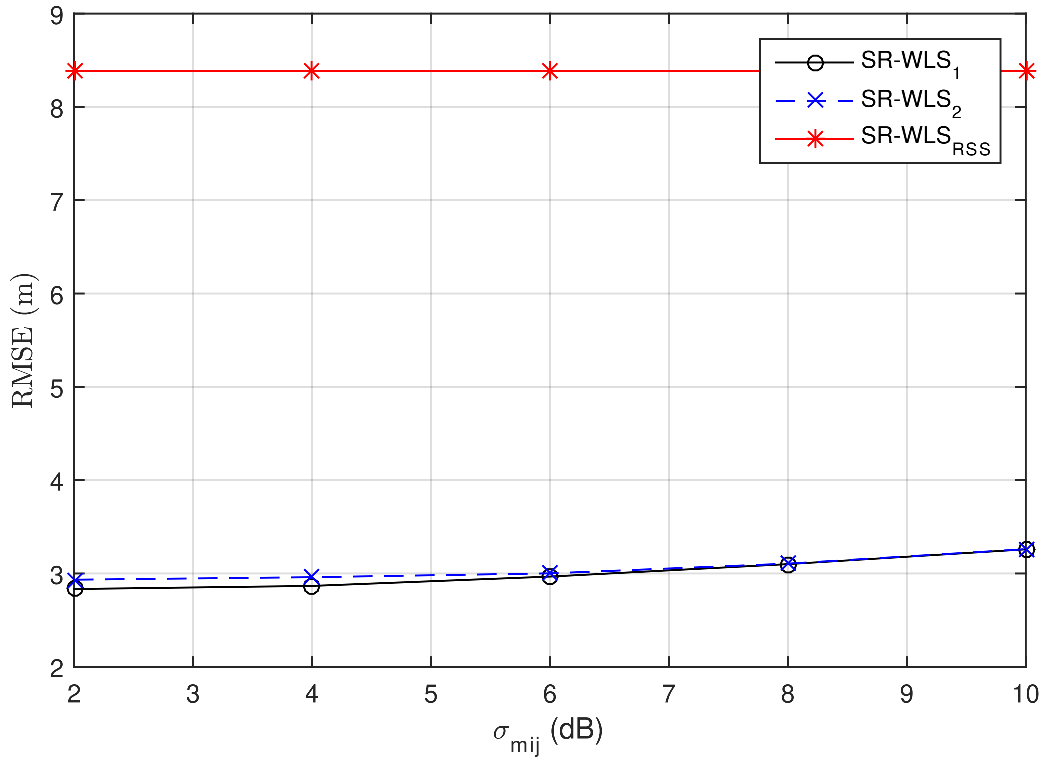

Figure 4.3: RMSE versus $\sigma_{m_{ij}}$ comparison

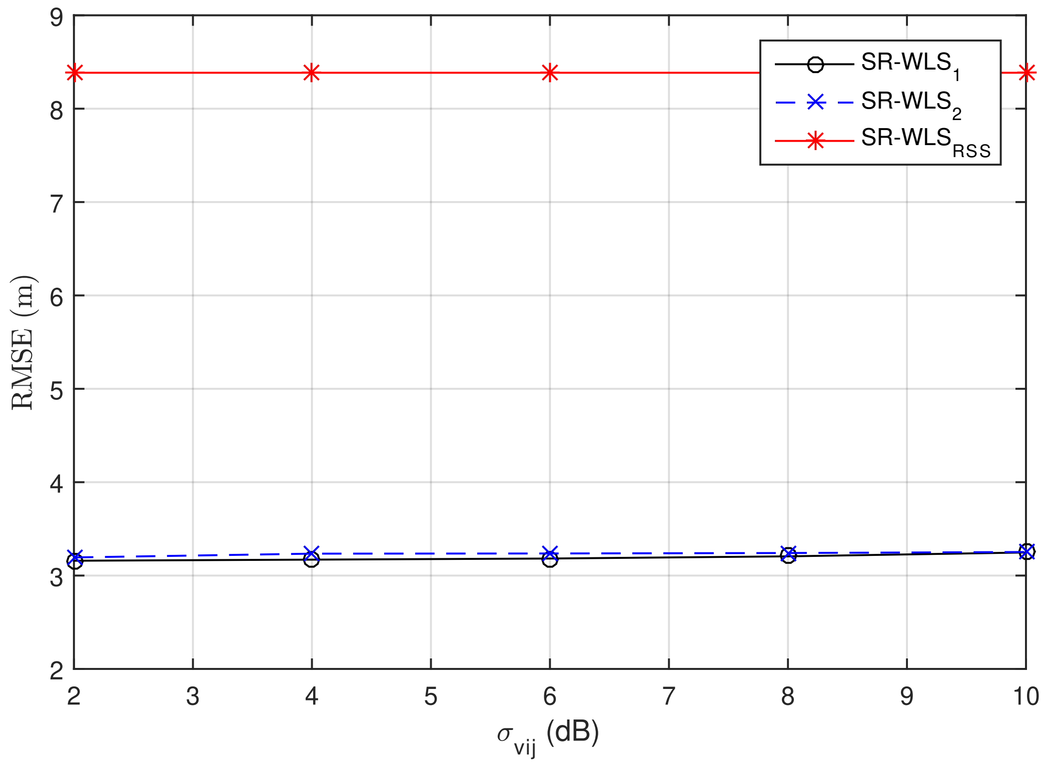

Figure 4.4: RMSE versus $\sigma_{v_{ij}}$ comparison

4.3.2 Cooperative Localization Results

For a cooperative WSN, comprehending targets and anchors, it is assumed that any sensor can communicate with another in its communication range (R) and all the targets location are estimated simultaneously. As has been already mentioned, this limited range forces a node cooperation to accomplish the main goal, obtaining the targets location. Unless stated otherwise, the communication range of any sensor is set to $R = 8$ meters which means that not all the targets may be in range with any other anchor in the network. In this type of scenario, it is known that the targets behave as pseudo-anchors, which means that in the simulations presented below it was considered that the radio measurements were also achieved by the targets. The number of Monte Carlo runs considered for each simulation was $M_c = 1000$ because this is a more complex scenario and the time of each simulation is significantly higher when compared to the time spent in simulations for the non-cooperative case.

In order to evaluate the performance of the considered algorithms, the metric used for this cooperative case was the normalized root mean square error (NRMSE), defined as follows:

$$NRMSE = \sqrt{\sum_{i=1}^{M_c} \sum_{j=1}^{M} \frac{\|x_{ij} - \hat{x}_{ij}\|^2}{M_c M}},$$

where $\hat{x}_{ij}$ represents the estimated location of the target x_j from the i-th M_c run.

In Fig. 4.5, the simulation results of the proposed SDP estimators as a comparison between the NRMSE and N, is shown. For such, the number of targets was set to twenty ($M = 20$) and the number of anchors varies from four to fourteen. As expected, and similarly to the non-cooperative case (Fig. 4.2), with the increasing number of anchors in the network the performance of the algorithms tends to improve. The decreasing gap between "SDP_1" and "SDP_2" occurs due to a better estimation of L_0 through eq. (3.36).

From this figure, it can be readily shown that the hybrid system, fusing two measurement types for this cooperative scenario, outperforms in a large scale a system using only RSS ("SDP_{RSS}").

In Fig. 4.6, the simulation results of a comparison made between the NRMSE and M are presented. The number of anchors equals to eight ($N = 8$) and the number of targets varies from five to twenty five. From this figure it can be seen that, adding more targets to the network while maintaining the same number of anchors does not compromise the performance of the considered approaches, in fact, it improves their performance. Another piece of data can be drawn from the observation of this figure is that, unlike Fig. 4.5, the gap between "SDP_1" and "SDP_2" rather than decreasing is slightly increasing. This would be expected and can be explained by the increasing number of targets in the network. When increasing the number of targets, keeping the same number of anchors, only unknown information is being added to the network impairing the estimation of L_0, used in "SDP_2".

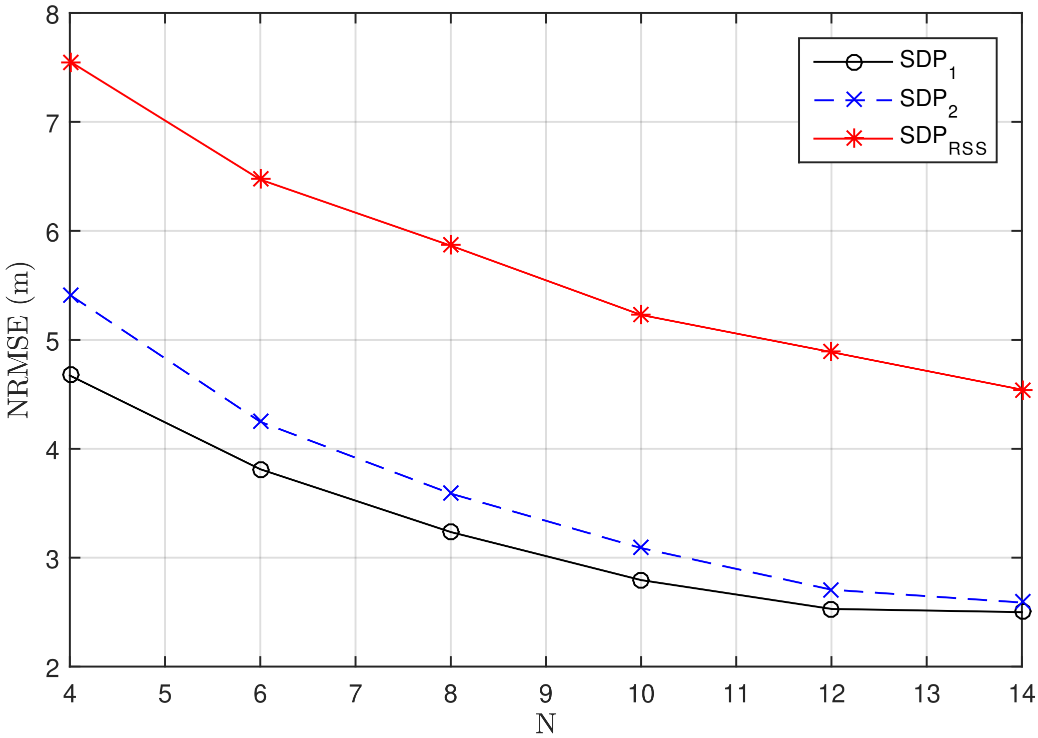

Figure 4.5: NRMSE versus N comparison

Although the gap between the proposed approaches does not reduce, the performance of the hybrid system continues to outperform the system using only one measurement type.

Fig. 4.7 illustrates the comparison of NRMSE with R of the proposed SDP estimators. For this simulation, the number os anchors and targets were, respectively, set to $N = 8$ and $M = 20$, and the range was varied from five to ten meters. From the figure it can be seen that, a five meter range is considered a critical value because it is where the hybrid system with unknown P_T ("SDP$_2$") has a worse performance than a system only using the RSS measurement with known P_T ("SDP$_{RSS}$"). This fact is easily explained by the fact that when the range is too low, there is no sufficient information available in the network to accurately calculate the targets location. On the other hand, increasing the range of the sensors, the hybrid system, with known and unknown P_T outperforms the the simpler system ("SDP$_{RSS}$") in an unequivocal manner. This behaviour is expected since from expanding the range leads to new connections for the sensors and for each additional connection, the hybrid system performs two measurements (RSS and AoA) while the other system only uses one measurement type (RSS).

It can also be observed, in Fig. 4.7, that, the bigger the range is, the more accurate targets location estimation can be. However, it is known that increasing the range affects directly the sensors lifetime. Because of this and depending on the application requisites,

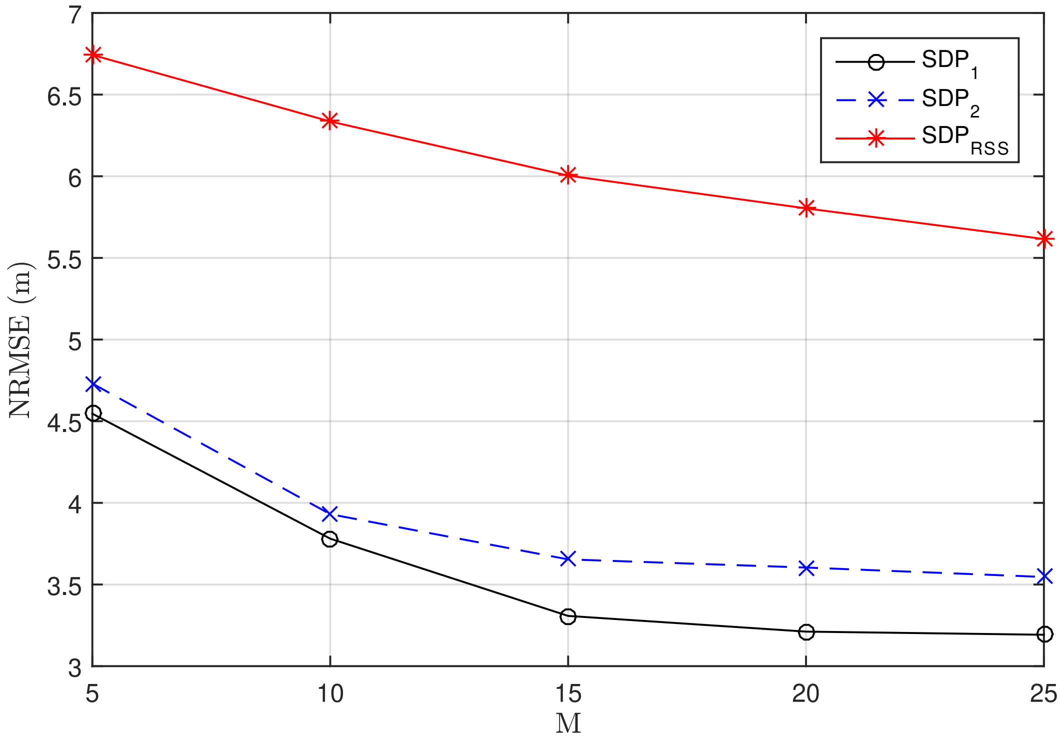

Figure 4.6: NRMSE versus M comparison

the best trade-off between the location accuracy and sensors lifetime should be obtained.

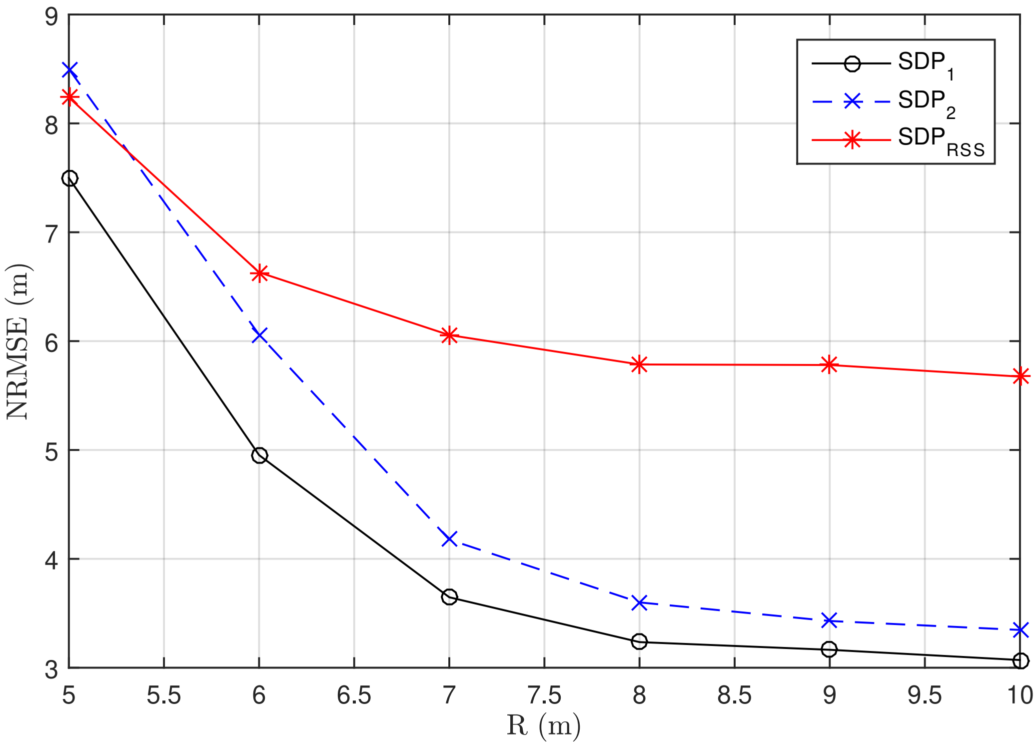

Figure 4.7: NRMSE versus R comparison

Chapter 5

Conclusions and Future Work

In the first part of this dissertation, the research motivations and the technical background that resulted in the different contributions of this work were presented. There was a brief discussion of WSNs issues. Having in mind these issues, the localization problem and the different methodologies to solve it were highlighted in the state of the art.

In Chapter 3 the implementation of the hybrid localization system fusing RSS and AoA measurements for 3-D WSNs was addressed, for the different cases. First a non-convex estimator based on the GTRS framework leading to a SR-WLS estimator was developed for the non-cooperative case with known P_T, followed by a generalization, to the case when the P_T was unknown, through the ML estimation of the unknown parameter, L_0. The remainder of this chapter was focused on the derivation of a convex SDP estimator to solve the cooperative localization problem. Similarly to the non-cooperative scheme, it was also shown that a straightforward generalization is possible between both cases of known to the unknown P_T, through the ML estimation of L_0.

Chapter 4 began with a computational complexity analysis of the considered estimators used through this dissertation. It was confirmed that the algorithms used in the cooperative localization were more computationally demanding then the others used for the non-cooperative. Since a cooperative localization problem is very challenging, requiring sophisticated mathematical tools in order to be solved efficiently and globally, this higher computational complexity was not a surprise. After this analysis, several simulations were performed in order to evaluate and investigate the performance of the proposed algorithms compared with an estimator using only RSS.

For the non-cooperative case, the evaluation metric used was the RMSE. It was proven that, for the considered scenarios and varying the errors parameters, the hybrid localization system outperforms significantly the system using only RSS. For the simulation where the number of anchors were varied it was seen that increasing the number of anchors benefits the estimation accuracy due to the fact that more reliable information is available. While with only three anchors in the network, the hybrid system, either with known and unknown P_T, showed errors smaller than four meters, the RSS system with known P_T, with eleven anchors in the network, presented errors above six meters. It was also shown that the major source of error is the RSS measurements. The errors associated to the angle measurements affect in a very small scale the location estimation process, namely the elevation angle which was simulated with a range of standard deviation from two to ten, and the error was always near to 3.22 meters.

In the cooperative localization problem case, the evaluation metric used was the NRMSE. The considered estimators showed a worse performance, in sense of estimation accuracy, when compared to the ones used in the non-cooperative case when the number of anchors were varied. This is not a surprise having in mind the different constraints which are present in this type of localization. As for example, in a non-cooperative scheme one target is located at a time and in a cooperative scheme all targets are located simultaneously. When maintaining all the variables untouched and increasing just the number of targets, it was seen that the hybrid system still outperforms the RSS system. However, the difference between the proposed estimators, with known and unknown P_T, increases with the increasing number of targets in the network. This fact occurs due to the fact that increasing this number of targets means that more unreliable information is added contributing to a worst ML estimation of L_0. In the last simulation it was seen that another major source of error is the intended range for each sensor. The difference in the range implies that more or less connections are available to each sensor. The selected range will depend on the number of sensors in the network, the estimation accuracy desired or the lifetime intended for each sensor since that increasing the range affects in a direct way the sensors battery.

With the conclusion of this dissertation is has been showed that for the simulations conditions, the performance results of the considered estimators were excellent and had robustness to not knowing P_T. However, it is worth mentioning that a simulation is not the real world and the estimation accuracy could vary depending on the environment conditions.

Based on the performance results observed in the simulations, it would be interesting to evaluate this performance with real sensors in different environments because the errors associated to the RSS and the AoA information will also depend on the specifications of each manufacturer of antennas and RSS indicators. It would be interesting to study hybrid systems fusing other types of measurement models.

Bibliography

[1] W. Dargie and C. Poellabauer. "Fundamentals of Wireless Sensor Networks". In: *Localization*. 2010, pp. 249–266.

[2] A. Goldsmith. *Wireless communications*. 2011, p. 827. ISBN: 9780470741863. DOI: 10.1002/9781119992806.fmatter. arXiv: arXiv:1011.1669v3.

[3] I. F. Akyildiz, S Weilian, Y Sankarasubramaniam, and E Cayirci. "Wireless sensor networks: A survey". In: *Computer Networks* 38 (2002), pp. 393–422.

[4] L. Gazzah, L. Najjar, and H. Besbes. "Selective Hybrid RSS/AOA Approximate Maximum Likelihood Mobile intra cell Localization". In: (2013).

[5] S. Wang, B. R. Jackson, and R. Inkol. "Hybrid RSS/AOA emitter location estimation based on least squares and maximum likelihood criteria". In: *2012 26th Biennial Symposium on Communications, QBSC 2012* (2012), pp. 24–29.

[6] L. Gazzah, L. Najjar, and H. Besbes. "Selective hybrid RSS/AOA weighting algorithm for NLOS intra cell localization". In: *IEEE Wireless Communications and Networking Conference, WCNC* (2014), pp. 2546–2551.

[7] A. Bahillo, S. Mazuelas, R. M. Lorenzo, P. Fern??ndez, J. Prieto, R. J. Dur??n, and E. J. Abril. "Hybrid RSS-RTT localization scheme for indoor wireless networks". In: *Eurasip Journal on Advances in Signal Processing* 2010 (2010).

[8] S Gowrishankar, T. G. Basavaraju, D. H. Manjaiah, and S. K. Sarkar. "Issues in wireless sensor networks". In: *Proceedings of the World Congress on Engineering*. Vol. 1. 2008, pp. 978–988.

[9] Eunchan Kim and Kiseon Kim. "Distance Estimation With Weighted Least Squares for Mobile Beacon-Based Localization in Wireless Sensor Networks". In: *IEEE Signal Processing Letters* 17.6 (2010), pp. 559–562.

[10] N. A. Alrajeh, M. Bashir, and B. Shams. "Localization techniques in wireless sensor networks". In: *International Journal of Distributed Sensor Networks* 2013 (2013).

[11] A. M. Youssef and M Youssef. "A Taxonomy of Localization Schemes for Wireless Sensor Networks." In: *Icwn* 9.8 (2007), pp. 1754–1757.

[12] S. Tomic, M. Beko, and R. Dinis. "RSS-based localization in wireless sensor networks using convex relaxation: Noncooperative and cooperative schemes". In: *IEEE Transactions on Vehicular Technology*. Vol. 64. 5. 2015, pp. 2037–2050.

[13] S. Tomic, M. Beko, and R. Dinis. "Distributed RSS-Based localization in wireless sensor networks based on second-order cone programming". In: *Sensors (Switzerland)* 14.10 (2014), pp. 18410–18432.

[14] T. He, C. Huang, B. M. Blum, J. a. Stankovic, and T. Abdelzaher. "Range-free localization schemes for large scale sensor networks". In: *Proceedings of the 9th annual international conference on Mobile computing and networking MobiCom 03* (2003), p. 81.

[15] S. P. Singh and S. Sharma. "Range Free Localization Techniques in Wireless Sensor Networks: A Review". In: *Procedia Computer Science* 57 (2015), pp. 7–16.

[16] D Niculescu and B Nath. "Ad-hoc Positioning System". In: *Proceedings IEEE GlobeCom* 1 (2001), pp. 25–29.

[17] N. Bulusu, J. Heidemann, and D. Estrin. "GPS-less low cost outdoor localization for very small devices". In: *IEEE Personal Communications, 7(5)* October (2000), pp. 28–34.

[18] R. Nagpal, H. Shrobe, and J. Bachrach. "Organizing a global coordinate system from local information on an ad hoc sensor network". In: *Information Processing in Sensor ...* (2003), pp. 1–16.

[19] T. Rappaport and Others. *Wireless communications: principles and practice*. Vol. 207. Prentice Hall, 1996.

[20] H Hashemi. "The indoor radio propagation channel". In: *Proceedings of the IEEE Vehicular Technology Conference (VTC 92)* (1992).

[21] T. S. Rappaport and L. B. Milstein. "Effects of radio propagation path loss on DS-CDMA cellular frequency reuse efficiency for the reverse channel". In: *Vehicular Technology, IEEE Transactions on* 41.3 (1992), pp. 231–242.

[22] N. Patwari, J. N. Ash, S. Kyperountas, A. O. Hero, R. L. Moses, and N. S. Correal. "Locating the nodes: Cooperative localization in wireless sensor networks". In: *IEEE Signal Processing Magazine* 22.4 (2005), pp. 54–69.

[23] G. Wang, H. Chen, Y. Li, and M. Jin. "On received-signal-strength based localization with unknown transmit power and path loss exponent". In: *IEEE Wireless Communications Letters* 1.5 (2012), pp. 536–539.

[24] R. M. Vaghefi, M. R. Gholami, R. Michael Buehrer, and E. G. Strom. "Cooperative received signal strength-based sensor localization with unknown transmit powers". In: *IEEE Transactions on Signal Processing* 61.6 (2013), pp. 1389–1403.

[25] D. C. Cox, R Murray, and A Norris. "800 {Mhz} Attenuation Measured in and around Suburban Houses". In: *At & T Bell Laboratory Technical Journal* 673.6 (1984).

[26] R. Bernhardt. "Macroscopic Diversity in Frequency Reuse Radio Systems". In: *IEEE Journal on Selected Areas in Communications* 5.5 (1987), pp. 862–870.

[27] R. W. Ouyang, A. K. S. Wong, and C. T. Lea. "Received signal strength-based wireless localization via semidefinite programming: Noncooperative and cooperative schemes". In: *IEEE Transactions on Vehicular Technology* 59.3 (2010), pp. 1307–1318.

[28] G. Wang, K. Yang, and A. O. Localization. "A New Approach to Sensor Node Localization Using RSS Measurements in Wireless Sensor Networks". In: *IEEE Transactions on Wireless Communications* 10.5 (2011), pp. 1389–1395.

[29] Kegen Yu. "3-D Localization Error Analysis in Wireless Networks". In: *IEEE Transactions on Wireless Communications* 6.10 (2007), pp. 3472–3481.

[30] Y. Wang and K. C. Ho. *An Asymptotically Efficient Estimator in Closed-Form for 3-D AOA Localization Using a Sensor Network.* 2015.

[31] A. N. Bishop, B. D. O. Anderson, B. Fidan, P. N. Pathirana, and G. Mao. "Bearing-only localization using geometrically constrained optimization". In: *IEEE Transactions on Aerospace and Electronic Systems* 45.1 (2009), pp. 308–320.

[32] A. Ozelci and R. Vinter. "The Shifted Rayleigh Filter for 3D Bearings-only Measurements with Clutter". In: *Information Fusion (FUSION), 2012 15th International Conference on* (2012), pp. 1385–1391.

[33] B. Laleh, H. Kennedy, and A. Finn. "Effects of Coordinate System Rotation on two Novel Closed-from localization Estimators Using Azimuth / Elevation". In: *Information Fusion (FUSION), 2013 16th International Conference on* (2013), pp. 1797–1804.

[34] L. Badriasl and K. Dogançay. "Three-dimensional target motion analysis using azimuth/elevation angles". In: *IEEE Transactions on Aerospace and Electronic Systems* 50.4 (2014), pp. 3178–3194.

[35] K. Dogançay. "3D pseudolinear target motion analysis from angle measurements". In: *IEEE Transactions on Signal Processing* 63.6 (2015), pp. 1570–1580.

[36] A. G. Lindgren and K. F. Gong. "Position and Velocity Estimation Via Bearing Observations". In: *IEEE Transactions on Aerospace and Electronic Systems* AES-14.4 (1978), pp. 564–577.

[37] H. J. Shao, X. P. Zhang, and Z. Wang. "Efficient closed-form algorithms for AOA based self-localization of sensor nodes using auxiliary variables". In: *IEEE Transactions on Signal Processing* 62.10 (2014), pp. 2580–2594.

[38] Z. Wang, J. A. Luo, and X. P. Zhang. "A novel location-penalized maximum likelihood estimator for bearing-only target localization". In: *IEEE Transactions on Signal Processing* 60.12 (2012), pp. 6166–6181.

[39] Q. Zhou and Z. Duan. "Weighted Intersections of Bearing Lines for AOA Based Localization". In: *Information Fusion (FUSION), 2014 17th International Conference on* Ml (2014), pp. 1–8.

[40] L. Lu and H. C. Wu. "Novel robust direction-of-arrival-based source localization algorithm for wideband signals". In: *IEEE Transactions on Wireless Communications* 11.11 (2012), pp. 3850–3859.

[41] J. Wang, J. Chen, and D. Cabric. "Stansfield localization algorithm: theoretical analysis and distributed implementation". In: *Wireless Communications Letters, ...* 2.3 (2013), pp. 327–330.

[42] N. Patwari. "Location Estimation in Sensor Networks". PhD thesis. The University of Michigan, 2005, pp. 1–205.

[43] G. Wang, H. Chen, Y. Li, and N. Ansari. "NLOS error mitigation for TOA-based localization via convex relaxation". In: *IEEE Transactions on Wireless Communications* 13.8 (2014), pp. 4119–4131.

[44] A. Bensky. *Wireless positioning technologies and applications*. 2008, p. 305.

[45] S. Tomic, M. Beko, and R. Dinis. "3-D Target Localization in Wireless Sensor Networks using RSS and AoA Measurements". In: *to appear in IEEE Transactions on Vehicular Technology* (2016).

[46] Y. T. Chan, F. Chan, W. Read, B. R. Jackson, and B. H. Lee. "Hybrid localization of an emitter by combining angle-of-arrival and received signal strength measurements". In: *Canadian Conference on Electrical and Computer Engineering* (2014).

[47] U. Hatthasin, S. Thainimit, K. Vibhatavanij, and N. Premasathian. "The use of RTOF and RSS for a one base station RFID system". In: *IJCSNS International Journal of Computer Science and Network Security* 10.7 (2010), pp. 184–195.

[48] T. Gadeke, J. Schmid, M. Kruger, J. Jany, W. Stork, and K. D. Muller-Glaser. "A bi-modal ad-hoc localization scheme for wireless networks based on RSS and ToF fusion". In: *2013 10th Workshop on Positioning, Navigation and Communication, WPNC 2013 - Proceedings* (2013).

[49] B. Zhang, J. Fan, G. Dai, and T. H. Luan. "A Hybrid Localization Approach in 3D Wireless Sensor Network". In: *International Journal of Distributed Sensor Networks* 2015 (2015).

[50] S. M. Kay. *Fundamentals of Statistical Signal Processing: Estimation Theory*. 1983.

[51] A. Beck and P. Stoica. "Exact and Approximate Solutions of Source Localization Problems". In: *IEEE Transactions on Signal Processing* 56.5 (2008), pp. 1770–1778.

[52] T. K. Pong and H. Wolkowicz. "The generalized trust region subproblem". In: *Computational Optimization and Applications* 58.2 (2014), pp. 273–322.

[53] J. J. Moré. "Generalization of the Trust Region Problem". In: *Optimization Methods and Software* 2 (1993), pp. 189–209.

[54] S. Tomic, M. Beko, and R. Dinis. "Distributed RSS-AoA Based Localization with Unknown Transmit Powers". In: *IEEE Wireless Communications Letters* (2016), pp. 1–1.

[55] S. Tomic, M. Beko, and R. Dinis. "Distributed Algorithm for Target Localization in Wireless Sensor Networks Using RSS and AoA Measurements". In: *submitted to Pervasive and Mobile Computing* (2016), pp. 1–24.

[56] S. Tomic, M. Beko, and R. Dinis. "A Closed-form Solution for RSS/AoA Target Localization by Spherical Coordinates Conversion". In: *submitted to IEEE Wireless Communications Letters* (2016).

[57] S. Boyd and L Vandendorpe. *Convex Optimization*. 2004.

[58] M Grant and S Boyd. "CVX: Matlab software for disciplined convex programming". In: *Available at http://cvxr.com/cvx/* (2008). URL: http://stanford.edu/{~}boyd/cvx.

[59] M. C. Grant and S. P. Boyd. "Graph implementations for nonsmooth convex programs". In: *Lecture Notes in Control and Information Sciences*. Vol. 371. 2008, pp. 95–110.

[60] F Zhang. *The Schur complement and its applications*. Vol. 4. 2005, p. 295.

[61] I. Polik and T. Terlaky. "Interior Point Methods for Nonlinear Optimization". In: *Nonlinear Optimization* 1989 (2010).

[62] J. F. Sturm. "Using SeDuMi 1.02, A Matlab toolbox for optimization over symmetric cones". In: *Optimization Methods and Software* 11.1-4 (1999), pp. 625–653.